A THESIS

FOR THE DEGREE OF MASTER OF SCIENCE

Molecular insights into pattern recognition and apoptosis in fish under pathological conditions through characterization of Toll-like receptor 2 and caspase 3 from Rock bream (*Oplegnathus fasciatus*)

Don Anushka Sandaruwan Elvitigala

Department of Marine Life Science

GRADUATE SCHOOL

JEJU NATIONAL UNIVERSITY

2013. 02

Molecular insights into pattern recognition and apoptosis in fish under pathological conditions through characterization of Toll-like receptor 2 and caspase 3 from Rock bream (*Oplegnathus fasciatus*)

Don Anushka Sandaruwan Elvitigala

(Supervised by Professor Jehee Lee)

A thesis submitted in partial fulfillment of the requirement for the degree of

Master of Science

2013. 02

This thesis has been examined and approved by

…….

Thesis Director

Choon Bok Song, Professor of Marine Life Science

……..

Joon-Bum Jeong, Professor of Marine Life Science

……

Jehee Lee, Professor of Marine Life Science

11.2012

Date

Department of Marine Life science

GRADUATE SCHOOL

JEJU NATIONAL UNIVERSITY

REPUBLIC OF KOREA

CONTENTS

요 약 문

분자유형 인식과 세포사멸기작(apoptosis)은 다양한 생물체에서 발생하는 기전으로 생체의 발생 및 분화에 중요한 역할을 한다. 최근의 연구들에 따르면 이 두 가지의 기전은 특히 세균감염에 있어 상호적인 관계가 있는 것으로 밝혀지고 있다. 감염의 확산을 막기 위해 침입 병원균 혹은 손상된 세포의 분자유형 인식은분자유형인식단백질들(pattern recognition proteins, PRRs)에 의해 각각 다른 면역signaling에 관계되는 분자들이 자극되어 downstream을 일으킴으로써 숙주방어기전인 apoptosis를 작동시키는 death cascade 라는 일련의 pathway를 자극시키는 다양한 면역신호를 시작하게 한다. 분자유형인식수용체와 관련하여, Toll-like receptors(TLRs)는 침입병원균을 다양한 범위에서 인식할 수 있는 분자로, PRR의 하위가계 단백질군 중 가장 초기에, 그리고 널리 알려져 있는 분자다. Apoptosis에서 시스테인계 아스파라산 단백질 분해효소(cysteine aspartic acid protease)인 caspase는 죽음신호(death signal)의 확산을 매개하는 중요한 분자로서 고려될 수 있다. 이러한 caspase중 caspase 3는 각각 다른 death signaling을 연결하여 직접적인 cell death를 일으키는 중추적인 역할을 하는 분자적 허브이다.

이 연구에서는 경제적으로 중요한 경골어류인 돌돔(Rockbream, *Oplegnathus fasciatus*)의 TLR 2(RbTLR2)와 caspase 3(Rbcasp3)의 유전자를 생리학적•병리학적인 상태일 때를 유전체 수준에서 분석하는 동시에 전사의 변화를 분석하였다. RbTLR2와 Rbcasp3의 완전한 게놈유전자의 서열은 random sheared bacterial artificial chromosome(BAC)를 이용하여 확인하였다. 그 후 확인한 서열은 생물정보학 프로그램을 이용하여 characterization을 하는 한편, 알려진 유사 서열과 비교를 위해 ClustalW를 사용, multiple alignment 및 pairwise를 수행하였다. 각각 두 유전자의 진화적인 위치를 확인하기 위해 다른 유사유전자들과의 계통수 조사도 이루어 졌다. 또한 엑손과 인트론으로 이루어진 게놈 구조를 확인하여 다른 종의 TLR 2 및 caspase 3 유전자들과 구조적 비교를 수행하였으며, 각각의 프로모터의 위치를 예측하여 잠재적인 전사인자로서 역할을 하는지 연구하였다. 그리고 돌돔의 caspase 3의 단백질 구조가 기능적인 면에서 어떠한 지를 알아보기 위해 I-TASSER와 RasMol2.7.5.2 프로그램을 이용하여 단백질 구조를 모델링, 확인하였다. 또한 재조합 단백질의 단백질 분해기능을 알아보기 위해 발현 벡터인 pMal-c2X에 Rbcasp3의 ORF를 클로닝하여 재조합 단백질을 분리, 정제하였다. 조직 특이적인 전사발현을 조사하기 위해 실시간 PCR(quantitative real-time PCR, qRT-PCR)을 수행하였고, 병원균 감염에 따른 간 조직에서의 전사발현 또한 조사하였다.

돌돔의 TLR 2와 caspase 3의 전체 cDNA의 길이는 4399 bp 및 2756 bp였으며, ORF의 길이는 각각 817개와 283개의 아미노산을 지정하는 2451 bp 및 849 bp로 나타났다. RbTLR2와 Rbcasp3의 단백질 크기는 각각 92 kDa 및 31 kDa으로 추측되었고 RbTLR 2가 signal peptide를 갖는 반면

Rbcasp3는 signal peptide를 갖지 않는 것으로 나타났다. RbTLR2는 전형적인 TLR 가계의 특징을 나타냈는가 하면, Rbcasp3는 독특한 caspase의 도메인 구조를 지녔다. 다른 종의 유전자간 identity와 similarity를 비교한 결과 RbTLR 2은 Orange spotted grouper(*Epinephelus coioides*)의 TLR 2와 , Rbcasp3의 경우 large yellow croaker (*Pseudosciaena crocea*)와 가장 높은 identity와 similarity를 보였다. Multiple alignment 결과, RbTLR2의 단백질 서열은 척추동물의 TLR 2유전자에서 공통적으로 보여지는 보존된 domain인 TIR domain이 C말단에 나타났고, Rbcasp3는 다른 caspase의 단백질서열에서 볼 수 있는 5개의 peptide와 RGD motif가 존재하는 것을 확인하였다. 계통수 조사에서는 RbTLR2는 척추동물군 중 orange spotted grouper와 가장 가까운 것으로 나타났고, Rbcasp3는 large yellow croaker와 진화적으로 가까운 위치를 차지하는 것으로 나타났다. 단백질의 3차구조 추정모델링은 사람 caspase 3의 삼차구조의 특징과 유사하게 나타났다.

두 유전자의 예측된 promoter 위치는 면역 신호에 있어 대부분 관계가 있는 데, 외•내적인 환경요인에 따라 전사조절이 매우 잘 통제가 되는 것으로 보여진다. RbTLR2의 gDNA의 길이는 10849로 10개의 인트론 사이에 11개의 엑손이 구조를 이루고 있었다. 반면에 Rbcasp3는 7529bp로 5개의 인트론과 6개의 엑손이 구조를 이루었다. 다른 어류의 gDNA구조와 배열해 본 결과, 상당한 상동성을 지녔다.

Rbcasp3 유전자는 pMal-c2X에 클로닝하여 BL21에 형질전환을 한 후 IPTG를 이용한 재조합 단백질의 발현을 유도하였다. 재조합된 단백질은 MBP단백질과 융합 및 발현되어 친화성 chromatography에 의해 정제되었고, 정제 caspase 3와 7 (DEVD-*p*NA)단백질의 caspase 8(IETD-*p*NA), caspase 9(LEHD-*p*NA)에 대한 기질 특이성 단백질분해활성실험을 수행하였다. 이 실험은 돌돔의 caspase3가 매우 유의적인 시스테인계 아스팔테이트 단백질에 대한 분해활성 기능을 지녔음을 시사한다.

RbTLR2와 Rbcasp3의 mRNA 발현양상 조사결과, 각각 신장과 혈구에서 높게 나타났다. 각 두 유전자의 감염에 따른 전사 양상은 돌돔의 간 조직에서 조사되었고, 면역 자극원 및 시간에 따라 전사가 많이 이루어졌다. *Streptococcus iniae* 는 RbTLR2의 전사발현을 현저히 높인 것으로 나타났다. 또한 *Edwardsiella tarda*와 LPS 역시 RbTLR2의 상당히 높은 전사를 유도한 것 ($P < 0.05$)으로 나타났다. 바이러스성 면역 자극원인 polyinosinic-polycytidylic acid(Poly I:C) 와 돌돔 바이러스인 이리도 바이러스(RBIV) 역시 RbTLR2의 발현을 증가시킨 것으로 나타났는데, 이는 경골어류에서 DNA virus가 PAMP로 인식할 수 있음을 처음으로 나타낸 결과이다. Rbcasp3의 경우 LPS에 의한 자극이 지속적인 발현증가를 유도하는 것으로 나타난 반면, *Edardsiella tarda*의 자극은 면역 자극 후반부에서 유의적이게 높은 발현을 나타냈다. 또한 돌돔 이리도 바이러스를 감염시켰을 때는 Rbcasp3가 면역 자극 후반부에서 높은 발현을 나타냈지만, 또 다른

바이러스성 면역 자극원인 Poly I:C의 경우 면역 자극 초반부에 높은 발현을 유도하는 것으로 나타났다.

이 연구는 돌돔을 모델로 하여 어류의 apoptosis와 분자유형인식과정에 중요한 역할을 하는 TLR2와 caspase3를 분자적인 관점에서 조사한 연구이다. 또한 이 연구는 현재 연구된 병원체 인식과 apoptosis의 면역 메커니즘에 대한 이해를 더욱 넓힐 것으로 예상되며 경골어류의 또 다른 면역 체계에 대한 연구를 수행하는 데에 도움이 될 것이다.

SUMMARY

Pattern recognition and apoptosis can be considered as significant bio-machineries in physiology of multicellular organisms which essentially contribute to their survival and development, even in the grievous environments. According to the recent reports, these two processes were found to be interrelated, especially in pathogenic infections. Upon the recognition of molecular patterns of invading pathogens and damaged cells, pattern recognition receptors (PRRs) can mount immune responses, via activating different downstream signaling molecules to initiate various immune signaling cascades, which can trigger the death cascade pathways to stimulate apoptosis as a host defensive mechanism to reduce the pool of infected cells, in order to restrict the propagation of the infection. With respect to the pattern recognition receptors, Toll-like receptors (TLRs) are known to be the initially discovered and extensively studied group of PRRs, which can interact with wide array of ligands in invaded pathogens. In terms of apoptosis, caspases as cysteine aspartic acid proteases can be considered as key molecular mediators to propagate the death signal through a cascade. Among them caspase 3 plays a pivotal role as a molecular hub in exclusionary phase of apoptosis by linking different death signaling pathways together to direct cells toward death.

In this study a novel counter parts of TLR 2 (RbTLR2) and Caspase 3 (Rbcasp3) genes, from an economically important teleost species, rock bream (*Oplegnathus fasciatus*), was characterized at genomic level, while analyzing their transcriptional modulation under physiological and pathological conditions. The complete genomic sequences of both RbTLR2 and Rbcasp3 genes were identified using a random sheared bacterial artificial chromosome (BAC) based gDNA library. Subsequently, the identified sequences were characterized using bioinformatics tools, while comparing the sequences with other known similitudes using

multiple and pairwise sequence alignment strategies of ClustalW software. In order to determine the evolutionary position of both molecules, phylogenetic relationship was determined with their known orthologues. Moreover, genomic organization of both Rbcasp3 and RbTLR2 as exons and introns was determined and compared with the known genomic architectures of their counterparts, further anticipating the respective promoter regions with their potential transcriptional factor binding sites. In addition, tertiary structure of Rbcasp3 was modeled using I-TASSER online server and visualized using RasMol 2.7.5.2 software to predict the structure-function relationship. Furthermore, Rbcasp3 complete coding sequence was cloned into pMAL-c2X expression vector and subsequently expressed and purified the recombinant protein to demonstrate the proteolytic activity of recombinant Rbcasp3 (rRbcasp3). The tissue specific transcriptional profile of both genes were determined using quantitative real time PCR (qRT-PCR), further analyzing their transcriptional regulation in liver tissues, upon the inductions with pathogenic stimulants and their molecular patterns.

The complete cDNA sequences of RbTLR2 (4399 bp) and Rbcasp3 (2756 bp) were consisted of 2451 bp and 849 bp coding sequences, encoding polypeptides of 817 and 283 amino acids, respectively. RbTLR2 was predicted to be comprised of a signal peptide whereas signal sequence was absent in Rbcasp3. Predicted molecular masses of RbTLR2 and Rbcasp3 were around 92 kDa and 31 kDa respectively. RbTLR2 resembled the typical TLR family signature whereas Rbcasp3 demonstrated the characteristic caspase domain architecture. TLR 2 orthologue of orange spotted grouper (*Epinephelus coioides*) exhibited the maximum identity and similarity values with RbTLR2. On the other hand, Rbcasp3 shared the highest sequence compatibility with its orthologue of large yellow croaker (*pseudosciaena crocea*). According to the multiple sequence alignment, C-terminal region of RbTLR2 including consensus sequences in TIR domain showed thorough conservation among its vertebrate counterparts and Rbcasp3 showed well conserved motifs among its orthologues, including

penta peptide motif and RGD motif. Phylogenetic analysis of RbTLR2 evidenced to its higher evolutionary proximity with orthologue from orange spotted grouper, among the other vertebrate similitudes, whereas Rbcasp3 demonstrated a closer evolutionary relationship with its caspase 3 homologue of large yellow croaker lying with in the fish clade. The modeled three dimensional structure of Rbcasp3 resembled the characteristic features of the folding of human caspase 3 tertiary structure, validating its *in-silico* derived primary structure.

Anticipated promoter regions of both RbTLR2 and Rbcasp3 genes consisting different transcriptional factor binding sites, most of which are related with immune signaling, revealed the tight regulation of their transcription by external and internal environmental factors. Moreover, genomic length of RbTLR2 was 10849 bp and genomic architecture was composed of multi-exonic structure, containing 11 exons interrupted by 10 introns. In contrast, Rbcasp3 was consisted of 6 exons, interrupted by 5 introns, expanded in 7529 bp genomic length. Arrangements at genomic level in both genes shared substantial compatibility with known genomic architectures of respective fish counterparts.

Rbcasp3 gene was cloned into pMAL-c2X, transformed into BL21 (DE3) cells and induced with IPTG to overexpress the proteins. The recombinant proteins were purified in MBP-fused form using an affinity chromatography and used in protease activity assay against caspase 3/7 (DEVD-*p*NA), caspase 8 (IETD-*p*NA) and caspase 9 (LEHD-*p*NA) specific substrates. Recombinant protein demonstrated a detectable and specific cysteine-aspartate protease activity against DEVD-*p*NA, convincing the functional viability of Rbcasp3.

RbTLR2 and Rbcasp3 demonstrated a different but ubiquitous transcriptional profile in tissues examined in healthy fish, where higher levels of mRNA were detected in spleen and liver, respectively. According to the immune challenge experiments in liver tissues of rock bream, transcription of both genes got up-regulated upon different stimuli, with the time.

Streptococcus iniae induction could boost RbTLR2 transcript level more prominently. Moreover, *Edwardsiella tarda* and LPS also significantly ($p < 0.05$) induced the transcription of RbTLR2 in liver tissues. On the other hand, two viral stimuli, polyinosinic-polycytidylic acid (poly I:C) and rock bream iridovirus (RBIV) could trigger the augmentation of RbTLR2, where the up-regulations upon RBIV convinces the recognition of PAMPs of DNA virus at the first time in teleosts. Stimulation with lipopolysaccharides (LPS) caused prolonged up-regulation of Rbcasp3 mRNA level, whereas *Edwardsiella tarda* stimulated its late-phase significant ($P < 0.05$) transcriptional induction. Rock bream iridovirus (RBIV) up-regulated Rbcasp3 transcription significantly ($P < 0.05$) at late-phase, however poly I:C induced the transcription of Rbcasp3 significantly at early-phase of the experiment.

Collectively, this study perceives molecular perspectives of apoptosis and pattern recognition of fish, considering rock bream as a model organism, while characterizing the crucial elements of respective processes, TLR2 and caspase 3. Moreover, this furnished a substantial contribution to the extension of existing knowledge on innate immune mechanisms, with respect to the pathogen recognition and apoptosis, emphasizing the requirement of further investigations and mining of different components of these processes in teleost species.

List of figures

List of Tables

INTRODUCTION

Rock bream as an aqua-crop

Mariculture is a branch of aquaculture, which is dedicated to cultivate marine organisms, especially for consumption as foods, since they are considered as a prominent substitution for terrestrial resources, regarding the fulfillment of daily nutritional requirements. Among those mariculture creatures, fish are used as the main delicacy in most parts of the world, prominently in East and South Eastern countries like China, Korea and Japan. Rock bream (*Oplegnathus fasciatus*) is an economically important comestible, harvested by commercial fisheries and mariculture farming inhabited in the coastal areas of the Pacific and Indian Oceans, accounting for a considerable yield as single species in the world marine aquaculture industry. However various pathogenic menaces, due to infections of bacteria like *Edwardsiella tarda* (*E. tarda*) and virus like rock bream iriodovirus (RBIV) have grievously affected to the reduction of the mariculture production of this aqua-crop, affirming the necessity of a precise disease management strategy in rock bream mariculture framing for its sustainability (Park, 2009; Zenke and Kim, 2008). According to this regard, investigation of immune mechanisms, functioning in rock bream is an effective approach to invent the appropriate preventive schemes. Since innate immune system is the fundamental defense mechanism in fish, which intern involve in stimulating the adaptive immunity, identification and revealing the roles of innate immune parameters will be a fruitful commencement in elucidating the different strategies of fish defense system (Magnadottir, 2006).

Toll-like receptors (TLRs) as the prominent pathogen sensors in innate immunity

Pattern recognition receptors (PRRs) are considered as key molecular guardians of innate immune system, naturally existing intracellularly or extracellularly, which are designed for recognizing non-self-molecules, mostly constituents of pathogenic organism, known as pathogen associated molecular patterns (PAMPs) and endogenous molecules released by stressed or damaged host cells, designated as damage associated molecular patterns (DAMPs) (Hansen et al., 2011). To date, wide array of PRRs have been identified and categorized into five groups, designated as, C-type lectins, Toll-like receptors (TLRs), retinoic acid inducible gene I (RIGI) like receptors (RLRs), the nucleotide-binding domain, leucine-rich repeat containing proteins (NLRs), and absent in melanoma (AIM)-like receptors (ALRs) (Hansen et al., 2011). Among them, TLRs are extensively studied group of PRRs, found in vertebrate as well as invertebrate linages in distinct forms, encoded by a multigene family.

TLRs are transmembrane proteins, consisting a characteristic common structure, including ectodomain, which is protruding outwards of the cell, composing 26 or lesser numbers of leucine rich repeat (LRR) motifs, transmembrane domain and endodomain in the cytoplasm containing Toll/interleukin (IL)-1 receptor domain (TIR) (Fig. 1.) (Palti, 2011).

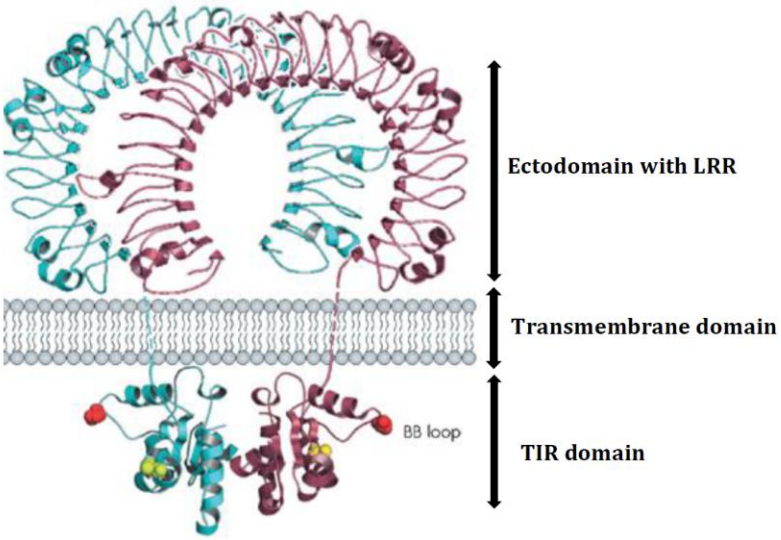

Fig. 1. Two TLR molecules expanded through cell membrane showing their basic domain architecture.

In human, 10 TLRs (TLR 1-10) have been identified to date, whereas in murine 12 TLRs were identified (1-9 and 11-13). Avians were known to be comprised 10 TLR types, 1, 2, 3-5, 7, 15, 16 and 21, including the paralouges of first two and last type (Hansen et al., 2011). Amphibians bear 20 distinct types of TLRs where most of them were evolutionary duplicated.(Hansen et al., 2011). Teleost TLRs show remarkable diversity among all other vertebrate species, comprising unique types, including TLR 20-23, which are known as non-mammalian TLRs, along with orthologs of above mentioned tetrapods, altogether representing 17 distinct TLR types. (Oshiumi et al., 2008; Rebl et al., 2010; Roach et al., 2005). However fish linages are lacking TLR 6 and 10 from mammalian similitudes. The structures of signaling molecules involve in downstream signaling of teleost TLR signaling cascades were found to be similar with mammalian counterparts and the regulation of immune responses were suggested to be analogous with that of mammals (Bricknell and Dalmo, 2005). Overall diversity of TLRs is attributed with recognition of distinct PAMPs by different TLRs. They can identify different components of pathogenic organisms, including

cell wall components of bacteria such as lipopolysaccharides (LPS) and lipoproteins, some proteins like flagellins and nucleic acids of bacteria or viral particles including dsRNA and dsDNA (Werling and Jungi, 2003).

Based on the ligand identified by the TLR, human TLRs can be classified into two major subfamilies. TLR 1, 2, 4, 5, 6 and 10 are capable of recognizing microbial lipids, sugars and proteins, categorized under cell surface subfamily, whereas TLR 3, 7, 8 and 9 responsible of recognizing nucleic acid derivatives of viral and bacterial origin are grouped under nucleic acid sensing subfamily (Palti, 2011).

TLR 2 as a crucial element in PAMP recognition

TLR 2 is known to form heterodimeric complexes with TLR 1 and TLR 6 to identify broad spectrum of PAMPs on Gram positive bacteria (Ribeiro et al., 2010). These receptor complexes can activate different transcriptional factors such as NF-κB through activating different downstream signaling molecules like myeloid differentiation primary response factor-88 (MyD88), to regulate the genes involve in innate and adaptive immunity (O'Neill and Bowie, 2007). Furthermore, TLR 2 was found to interact with variety of additional ligands including zymosans, a derivative from yeast, glycosylphoshatidylinositols (GPIs) from protozoan parasites and LPS of gram negative bacteria (Hirschfeld et al., 2001; Underhill et al., 1999; Werts et al., 2001). Interestingly, TLR 2 also can recognize PAMPs on Gram negative bacteria, either with TLR 4 (Hadley et al., 2005) or independently (O'Connell et al., 2006). As an exceptional finding, a viral dsRNA mimic (poly I:C) recognition potency of TLR 2 was noticed from Japanese flounder, revealing a novel and potent TLR 2 agonist of teleost fish (Hirono et al., 2004). TLR 2 was already characterized and its expression profile was reported in several teleost fish species, including fugu (Oshiumi et al., 2003), zebrafish (Jault et al., 2004; Meijer et al., 2004) Japanese flounder (Hirono et al., 2004), catfish

(Baoprasertkul et al., 2007) and rohu (Samanta et al., 2012). In addition TLR 2 from orange spotted grouper was characterized with TLR 1, as a combinative study (Wei et al., 2011).

In order to extend the available knowledge on TLR 2 of teleosts, herein TLR 2 was characterized from rock bream (*Oplegnathus fasciatus*) (RbTLR2), revealing its complete genomic structure and profiling its transcription in healthy and immune challenged fish, upon *Edwardseilla tarda* (*E. tarda*), *Streptococcus iniae* (*S. iniae*), Lipopolysaccharides (LPS), polyinosinic:polycytidylic acid (poly I:C) and Rock bream irido virus (RBIV), convincing their potential involvement in host antiviral and antibacterial defense.

Apoptosis at a glance

Development of a multicellular organism highly depends on the equilibrium of cell proliferation and cell death, which are known to be tightly regulated processes by different mechanisms. Programmed cell death (PCD) is one of those mechanisms which can effectively balance the life and the death of cells (Danial and Korsmeyer, 2004). Among different PCD types, apoptosis is considered as a key component which occurs normally during development and aging and as a homeostatic mechanism to maintain cell populations in tissues (Elmore, 2007). Moreover, apoptosis was known to be mounted as a host defense mechanism through mediating immune responses, especially immune responses mount against viral infections (Everett and McFadden, 1999; Sun and Shi, 2001) and counterbalancing the consequences of pathological conditions (Norbury and Hickson, 2001). In general, apoptosis is characterized by wide array of biochemical events occur in cells including protein cleavage, protein cross-linking, DNA breakdown, and morphological changes such as shrinkage of the cell, condensation of chromatin, and disintegration of the cell into small fragments (so-called ‘‘apoptotic bodies’’) that can be removed by phagocytosis (Hengartner, 2000; Kerr et al., 1972).

There are basically two main path ways of apoptosis, designated as extrinsic or death receptor mediated pathway and intrinsic or mitochondria mediated pathway (Igney and Krammer, 2002). In addition, another pathway which involves T-cell mediated cytotoxicity and perforin-granzyme-dependent killing of the cell was already identified in animals (Igney and Krammer, 2002). However these three pathways are linked together at the same terminal, rendering the activation of the executionary phase of the apoptosis (Elmore, 2007).

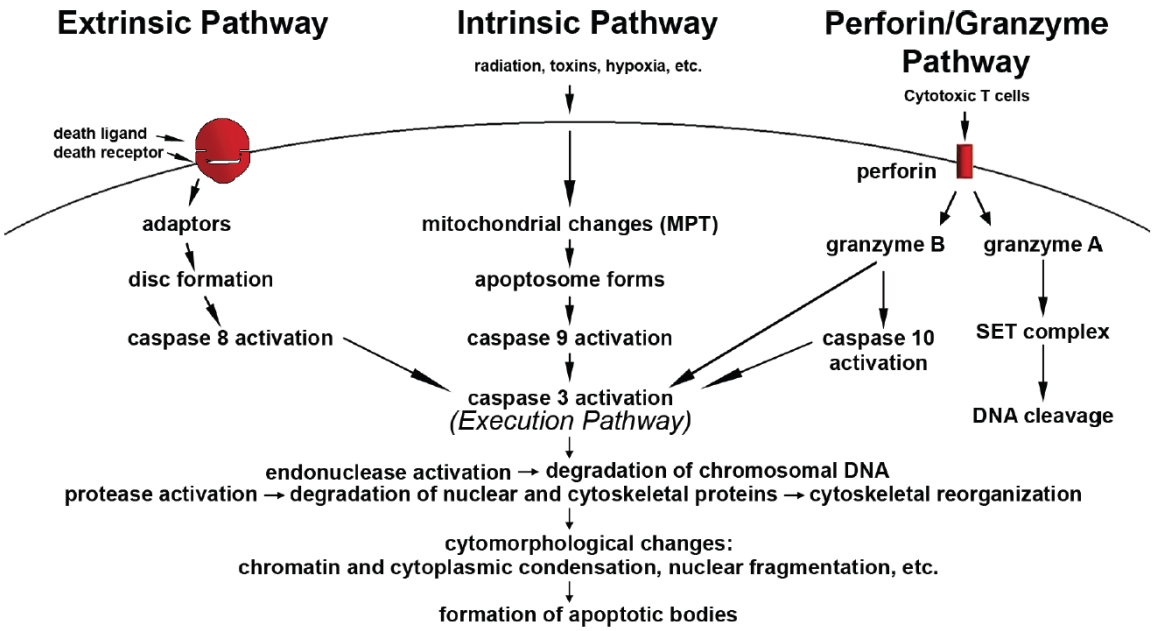

Fig. 2. Schematic representation of apoptotic pathways with their key members.

Caspase 3 as a key mediator of apoptosis

Host-encoded caspases are considered as the primary regulators of apoptosis (Cohen, 1997; Nicolson, 1999; Thornberry and Lazebnik, 1998). Caspases are an evolutionarily conserved family of **c**ysteine **a**spartic **s**pecific **p**rote**ase**s responsible for a diverse array of cellular functions, the well-recognized of which are apoptosis and inflammation. In pre-apoptotic cells, caspases exist as inactive pro-enzymes (zymogenes) (Ganesan et al, 2006) which mainly consist of three distinct domains: a pro-domain, followed by a large subunit and a small subunit. The latter two subunits are connected by a linker region, which itself is flanked by aspartic acid residues (Nicolson and Thornberry, 1997).

Caspases can be self-activated or be activated by upstream-caspase proteases in death cascade that cleaves conserved aspartic acids in the C terminal region. (Fuentes-Prior and Salvensen, 2004). To date, 11 human caspases have been identified and functionally categorized into two groups; inflammatory caspases and apoptotic caspases. The latter has been further divided into initiators and effectors (Nicolson, 1999). The effector caspases (caspase 1, 3, 4, 5, 6, 7, and 11) are activated by the self-activated initiator caspases, which function in the upstream of the apoptotic signaling pathway (Ho and Hawkins, 2005; Miao et al, 2010). Caspases and caspase-like enzymes have also been identified in non-metazoans, such as plants, fungi, and prokaryotes (Boyce et al, 2004). Caspases are regulated at several stages, such as at the transcriptional and post-transcriptional levels (Earnshaw et al, 1999). Moreover, enzymatic activity of caspases can be inhibited by members of a conserved family of proteins known as inhibitor of apoptosis (IAP) factors (Deveraux and Reed,1999).

Caspase 3, one of the effector caspases, is involved in executing the cell death signaling cascade of intrinsic and extrinsic apoptotic pathways, following its activation by caspase 8 and caspase 9, respectively (Lavrik et al, 2005). Activated caspase 3 mediates many of the

characteristic morphological alterations of apoptosis, such as break-down of several cytoskeletal proteins, cleavage of polyadenosine dipeptide ribose polymerase (PARP) and degradation of the inhibitor of caspase-activated DNAses (ICADs), resulting in the release of CAD to cleave cell DNA and ultimately directing the cell toward death (Cohen, 1997).

Caspase 3 has been identified and characterized in several teleost fish species; Studies of caspase 3 homologues in European sea bass (*Dicentrarchus labrax*), zebrafish (*Danio rario*), large yellow croaker (*Pseudosciaena crocea*), and Atlantic salmon (*Salmo salar*) have revealed an immune-related functions in these fishes (Li et al, 2011; Reis et al, 2007; Takle et al, 2006; Yabu et al, 2001). Furthermore, two isoforms of caspase 3 (A and B) have been identified in medaka *(Oryzias latipes*) (Naruse et al, 2000) and Atlantic salmon (Takle et al, 2006).

In this study, rock bream caspase 3 (Rbcasp3) was identified and characterized the at transcriptional and genomic levels. We determined the basal tissue distribution and transcriptional response in liver tissue to immune challenges with LPS, *E. tarda*, RBIV and poly I:C. We not only demonstrated that Rbcasp3 harbors immune-related hydrolytic activity using recombinant protein, but also determined that apoptosis represents an immune responsive process in rock bream.

Chapter I

A teleostean counterpart of TLR 2 from rock bream (*Oplegnathus fasciatus*): Genomic characterization and expressional profile under pathological conditions

1. ABSTRACT

Toll-like receptors (TLRs) are well characterized pattern recognition receptors, responsible of initiating immune responses, through the recognition of various types of pathogen associated molecular patterns (PAMPs). TLR 2 is one variant among a wide array of existing types of TLRs, which mostly trigger immune responses by recognizing bacterial cell wall components, while activating the downstream molecules of the signaling cascade, such as MyD88. In this study TLR 2 from rock bream; *Oplegnathus fasciatus* (RbTLR2) was identified and characterized in genomic level. The complete coding sequence of RbTLR2 was 2451 bp in length, encodes an 817 amino acid peptide with a calculated molecular mass of 92.3 kDa. The deduced protein followed the typical TLR domain architecture, containing leucine rich repeats (LRR) and toll-interleukin receptor domain (TIR). The genomic length of RbTLR2 was 10849 bp, containing eleven exons, interrupted by 10 introns. The phylogenetic analysis depicted a high evolutionary proximity with its vertebrate counterparts, especially with those of piscines. Several important transcription factor binding sites, including sites that interact with immune signals, were identified in anticipated promoter sequence using *in-silico* analysis. The quantitative real time PCR detected a ubiquitous transcription of RbTLR2 in selected rock bream tissues, where more pronounced expression levels were reported in spleen and liver. Differential transcriptional modulation of RbTLR2 was observed in rock bream liver tissue upon five different immune inductions, where *Streptococcus iniae* induction could boost its transcript level more prominently. Moreover *Edwardsiella tarda*

and Lipopolysaccharides (LPS) also induced the transcription of RbTLR2 in liver tissues, significantly ($p < 0.05$). On the other hand, two viral stimuli, poly I:C and rock bream iridovirus (RBIV) could trigger the augmentation of RbTLR2, where the up-regulations upon RBIV, convinces the recognition of PAMPs of DNA virus at the first time in teleosts. Collectively, our findings support us to suggest that RbTLR2 may play a significant role in host antiviral and antibacterial defense in rock bream.

2. MATERIALS AND METHODS

2.1. Rock bream cDNA library construction and identification of partial cDNA sequence of RbTLR2

A rock bream sequence data base was established using the Roche 454 genome sequencer FLX systems (GS-FLX^{Tm}), a next generation DNA sequencing (NGS) technology (DNA Link, Republic of Korea). Briefly, total RNA was isolated using Tri Reagent^{TM} (Sigma, USA) from several tissue pools including gills, blood, liver, spleen, pituitary gland, head kidney and kidney of three healthy rock bream fish. Subsequently, the mRNA was purified using an mRNA isolation kit (FastTrack® 2.0, Invitrogen, USA). The first strand cDNA synthesis and normalization were carried out with the Creator^{TM} SMART^{TM} cDNA library construction kit (Clontech, USA) and Trimmer-Direct cDNA normalization kit (Evorgen, Russia). Thereafter, the GS-FLX^{TM} sequencing of rock bream cDNA was performed according to the manufacturer's instructions (Roche Applied Science, USA). Using the Basic Local Alignment Tool (BLAST) algorithm (http://www.ncbi.nlm.nih.gov/BLAST), TLR 2 Partial length cDNA sequence in rock bream sequence data base was identified.

2.2. Identification of complete genomic sequence of RbTLR2

A random shear bacterial artificial chromosome (BAC) library of Rock bream genomic DNA was custom constructed and DNA containing clones were arranged into pools and super pools (Lucigen, USA). RbTLR2 gene was screened using this gDNA library, by Polymerase chain reaction (PCR), using sequence specific primer pair, RbTLR2-F and RbTLR2-R (Table 1), as described previously (Quiniou et al., 2003). The Primers were designed based on previously identified RbTLR2 (section 2.1) partial cDNA sequence. The PCR was employed in TaKaRa thermal cycler in a total volume of 20 µl with 0.5 U of Ex Taq polymerase (TaKaRa, Japan), 2 µl of 10x Ex Taq buffer, 1.6 µl of 2.5 mM dNTPs, 75 ng

of template and 10 pmol of each primer. The reaction was carried out with an initial incubation at 94°C, followed by 35 cycles of 94°C 30 s, 58°C 30 s and 72°C 30 s. The PCR products were analyzed on a 1.5% agarose gel and based on the appearance of the band; Putative clone, containing TLR 2 gene was correctly located. Subsequently, detected clone was sequenced (GS-FLX^{TM}), in order to obtain the genomic DNA sequence of RbTLR2 gene. ORF of RbTLR2 was identified by NCBI-BLAST algorithm (http://www.ncbi.nlm.nih.gov/BLAST) from the above confirmed genomic DNA sequence. The nucleotide sequence of the RbTLR2 was deposited in GenBank under the accession No. JX025020.

2.3. Sequence characterization and phylogenetic analysis

The orthologous sequences of RbTLR2 were compared by BLAST search program. Pairwise sequence alignment (http://www.Ebi.ac.uk/Tools/emboss/align) and multiple sequence alignment (http://www. Ebi.ac.uk/Tools/clustalw2) were performed using the ClustalW2 program. The phylogenetic relationship of RbTLR2 was determined by Neighbor-Joining method, using Molecular Evolutionary Genetics Analysis (MEGA) software version 3 (Kumar et al., 2004). Prediction of protein domains was carried out using the ExPASy-PROSITE data base (http://prosite.expasy.org), SMART online server (http://smart.embl-heidelberg.de) and MotifScan scanning algorithm (http://myhits.isb-sib.ch/cgi-bin/motif_scan). Furthermore, signal peptide was predicted using signalP server (http:www.cbs.dtu.dk/service/signalP) and some physicochemical properties of deduced protein was predicted using ExPASy prot-param tool (http://web.expasy.org/protparam).

Genomic sequence of RbTLR2 identified from BAC clone was used to identify the exon-intron structure and predict the promoter region, along with potential transcriptional factor binding sites. The transcription initiation site (TIS) was predicted using online neural network

promoter prediction tool from Berkekey Drosophila Genome Project (Reese, 2001) and potential cis acting elements around 1kb upstream of the TIS was detected using TFSARCH ver.1.3 and Alibaba 2.1 software.

2.4. Experimental fish and tissue collection

Rock bream, with an average body weight of 50 g were obtained from the Jeju Special Self-Governing Province Ocean and Fisheries Research Institute (Jeju, Republic of Korea). The fish were maintained in a controlled environment at 22-24 °C. All individuals were allowed to acclimate for two weeks prior to experimentation. Whole blood (1 ml per fish) was collected from the caudal fin using a sterilized syringe, and the sample was immediately centrifuged at 3,000 x g for 10 min at 4 °C to separate the blood cells from the plasma. The collected cells were snap-frozen in liquid nitrogen. Meanwhile, the fish was sacrificed and the gill, liver, skin, spleen, head kidney, kidney, skin, muscle, brain and intestine were excised and immediately snap-frozen in liquid nitrogen and stored at -80 °C.

2.5. Immune challenge experiment

In order to determine the immune responses of RbTLR2, pathogenic bacterium *E. tarda*, *S. iniae*, RBIV, poly I:C and LPS were used as immune-stimulants in time course experiments. Each rock bream was administered a single intraperitoneal (i.p.) injection of 100 μL LPS in phosphate buffered saline (PBS) suspension (1.25 μg/μL, *E. coli* 055:B5; Sigma) or 100 μL poly I:C in PBS suspension (1.5 μg/μL; Sigma). For the bacterial-challenge experiment, *E. tarda* and *S. iniae* were obtained from the Department of Aqualife Medicine, Chonnam National University, Korea. The bacteria were incubated at 25 °C for 12 h using a brain heart infusion (BHI) broth (Eiken Chemical Co., Japan) supplemented with 1% sodium chloride. The cultures were resuspended in sterile PBS, and then diluted to a desired concentration. Each rock bream was Intraperitonealy injected with 100 μL live *E.*

tarda in PBS (5×10^3 CFU/mL) or 100 μL live *S. iniae* in PBS (1×10^5 CFU/mL). For the virus challenge experiment, kidney tissue specimens obtained from the moribund rock bream infected with rock bream iridovirus (RBIV) were homogenized in 20 volumes of PBS. The tissue homogenate was centrifuged at 3000 × g for 10 min at 4 °C, and the supernatant of a RBIV sample was filtered through a 0.45 μm membrane. Each rock bream was then infected with a single i.p. injection of 100 μL RBIV in PBS. A control group was injected with an equal volume (100 μL) of PBS. Rock bream liver samples were collected at 3, 6, 12, 24 and 48 h post-injection (p.i.) from LPS-, poly I:C, *E. tarda*, *S. iniae* or RBIV-infected rock breams as described in section 2.4. PBS-injected samples (positive control) were also isolated at each time point from 3 h p.i to 48 h p.i. and a group of three un-injected animals were served as a negative control. Three rock breams were obtained for each time point and the pooled tissues from each group were subjected to total RNA extraction and cDNA synthesis.

2.6. Total RNA extraction and cDNA synthesis

Total RNA was extracted from each of the excised tissues by using the Tri Reagent™ (Sigma-Aldrich, USA). Concentration of RNA was determined at 260 nm in a UV-spectrophotometer (Bio-Rad, USA) and diluted to 1 μg/μL. 2.5 μg of RNA from selected tissues was applied in cDNA synthesis using cDNA synthesis kit (TaKaRa, Japan) according to the manufacturer's instructions. Finally, the newly synthesized cDNA was diluted 40-fold (total 800 μl) and stored at -20 °C until needed for further analysis.

2.7. RbTLR2 mRNA expression analysis by quantitative real time polymerase chain reaction (qRT-PCR)

qRT-PCR was used to detect the expression levels of RbTLR2 in the above mentioned tissues (section 2.6) and the temporal expression of RbTLR1 in liver (RbMyD88), after challenged by different PAMPs and microorganisms mentioned in section 2.5. Total RNA was extracted at different time points following immune stimulation, and the first strand cDNA synthesis was carried out as described in section 2.6. qRT-PCR was carried out using a Thermal Cycler Dice^{TM} (Real Time System TP800; TaKaRa, Japan) in a 15 µl reaction volume containing 4 µl of diluted cDNA from each tissue, 7.5 µl of 2x TaKaRa Ex TaqTM, SYBR premix, 0.5 µl of each primer (RbTLR2-F and RbTLR2-R-Table 1) and 7.5 µl of double distilled H_2O. The qRT-PCRs were performed under following conditions: 95°C for 10 seconds, then 35 cycles of 5 seconds at 95 °C, 10 seconds at 58 °C and 20 seconds at 72 °C and final cycle of 95 °C for 15 seconds, 60 °C for 30 seconds and 95 °C for 15 seconds. The base line was set automatically by the Thermal Cycler Dice^{TM} Real Time System Software (version 2.00). RbTLR2 expressions were determined by the Livak ($2^{-\Delta\Delta CT}$) method (Livak and Schmittgen, 2001). The same qRT-PCR cycle profile was used for the internal reference gene, rock bream β-actin (Genbank ID: FJ975146) using the corresponding sequence specific primer pair (Table 1). Each analysis was carried out in three replicates. All data are presented as relative mRNA expression as means ± standard deviation (SD). To determine statistical significance ($p < 0.05$), two tailed paired T test was carried out.

Tabel 1. Primers used in the study on RbTLR2

Name	Purpose	Sequence (5' →3')
RbTLR2-F	BAC library screening and qRT-PCR of RbTLR2	TGTCTCCACAAACGGGACTTCCTT
RbTLR2-R	BAC library screening and qRT-PCR of RbTLR2	GTCGGACTGGACAAAGTTCTCTGA
Rb-βF	qRT-PCR for rock bream β-actin gene	TCATCACCATCGGCAATGAGAGGT
Rb-βR	qRT-PCR for rock bream β-actin gene	TGATGCTGTTGTAGGTGGTCTCGT

3. RESULTS AND DISCUSSION

3.1 Sequence characterization and phylogenetic analysis

The complete cDNA sequence of RbTLR2, derived through assembling approach of the predicted exons, according to the canonical AG/GT rule, consisted of 4399 nucleotides, comprising of a 2451 bp open reading frame (ORF), encoding 817 amino acids, 535 bp 5' untranslated region (5' UTR) and 1412 bp 3' UTR. Predicted molecular mass of RbTLR2 was around 92.3 kDa which lies within the generally accepted molecular mass range of TLRs (90-115 kDa) (Bell et al., 2003) and theoretical isoelectric point was 6.03.

Overall protein sequence of RbTLR2 resembled the typical TLR domain architecture, basically comprising of ectodomain with 9 LRR motifs (residues 79-100, 101-130, 150-173, 174-197, 360-384, 389-411, 459-484 and 479-502) including C-terminal LRR module (536-591), transmembrane domain (residues 593-615) and endodomain containing TIR (residues 653-812) as predicted by SMART online server. In addition, according to the *in-silico* prediction, first 20 amino acids represented the signal peptide of RbTLR2, which is important for the extracellular localization of TLRs (Fig. 3).

As a principle, large surface area of TLR ectodomain facilitates the interaction of different ligands with TLRs, providing a partial elucidation to the broad specificity of some TLRs to PAMPs. Number of LRR motifs in the ectodomain can be considered as one of the important factors which contribute to the increased surface area (Bell et al., 2003). According to the domain architecture comparison among different vertebrate species (Fig. 3), it can be clearly observed that ectodomains of mammalians, such as human and mouse as well as teleost (rock bream, fugu and orange spotted grouper) TLR 2 similitudes are comprised of higher numbers of LRRs compared to other species in different taxonomic

classes considered. This characteristic feature may contribute to the multi-ligand identification, as reported previously (Palti, 2011; Rebl et al., 2010; Xagorari and Chlichlia, 2008).

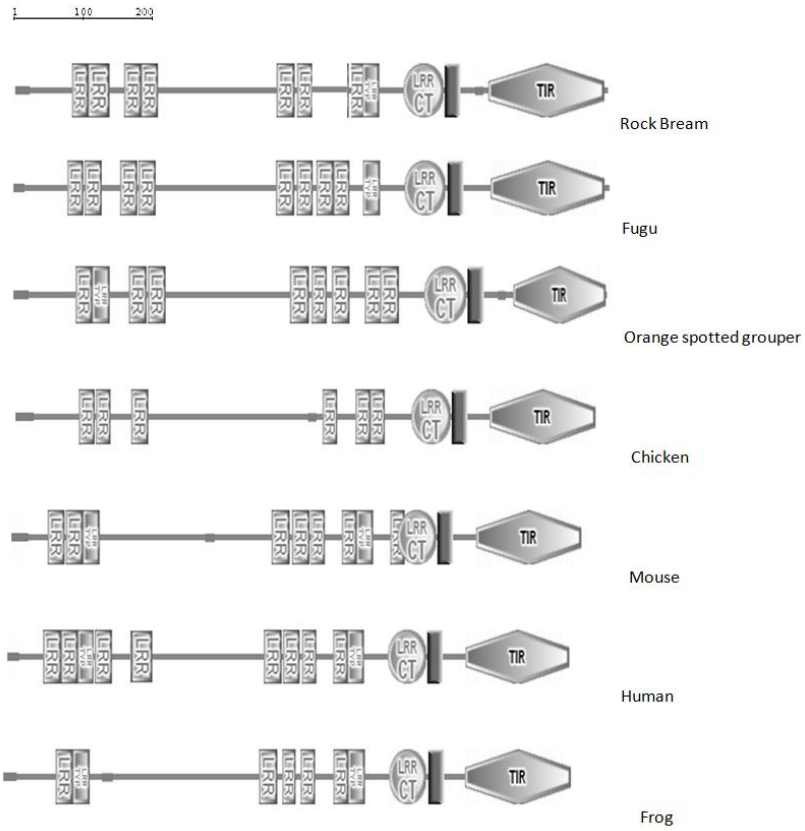

Fig. 3. Schematic structures of TLR 2 from different vertebrate species. Structures obtained from the SMART analysis (at ExPASy web server) of the amino acid sequence from rock bream, fugu, orange spotted grouper, chicken, mouse, human and frog TLR 2. Small horizontal boxes at the starting of the structures represent the signal peptide, where vertical light gray boxes depict the LRR motifs. C-terminal LRR is indicated by LRR-CT using an oval. Dark gray boxes represent the transmembrane domains.

The pairwise sequence alignment, performed by ClustalW2 program revealed that the complete RbTLR2 protein sequence and its TIR domain are sharing different identity and similarity percentage values with wide array of species, where significantly high

compatibility was observed with piscines (Table 2). With respect to entire protein sequence, RbTLR2 exhibited percentage identities in 81%-19.7% range, highest with orange spotted grouper and lowest with sea squirt. Similarly, regarding the TIR domain of RbTLR2, identity percentage lie between 88.1% - 30.1%, where the highest and the lowest were reported with the counterparts of same species reported in the complete sequence comparison of RbTLR2. Hence, both observations affirm that RbTLR2 is a TLR 2 orthologue. Nevertheless, TIR domain of RbTLR2 shared relatively prominent percentage identities and similarities, compared to those of RbTLR2 entire sequence in almost all the alignments, indirectly convincing the greater compatibility of endodomains compared to ectodomains of TLR 2 variants. This observation reflects that similar signaling pathways can be triggered by different PAMPs of TLR 2, as endodomains are dedicated to initiate the signaling cascades upon identification of respective PAMPs by ectodomains of TLRs (Bell et al., 2003; Slack et al., 2000).

Table 2. The percentage similarities and identities of RbTLR2 gene and its TIR domain, with TLR 2 and their respective TIR domains of other species. Accession numbers of frog and sea squirt TLR 2 proteins were obtained from Ensemble and EMBL data bases respectively and remaining were extracted from NCBI-GenBank sequence data base.

aa- amino acids, **I**-identity, **S**- Similarity

	Entire sequence				TIR		
Name of the species	**Accession number**	**a.a**	**I(%)**	**S (%)**	**a.a**	**I (%)**	**S (%)**
Epinephelus coioides (orange-spotted grouper)	AEB32453	824	81.0	88.8	160	88.1	93.8
Trematomus bernacchii(emerald rockcod)	ACT64128	804	77.3	85.9	157	87.5	91.9
Chionodraco hamatus (icefish)	ACT64127	802	77.1	86.0	157	85.6	91.2
Paralichthys olivaceus (Japanese flounder)	BAD01044	818	76.2	84.8	160	85.6	93.8
Takifugu rubripes (Fugu)	AAW69370	810	67.1	79.2	156	67.1	79.2
Ictalurus punctatus (catfish)	AEI59663	790	47.2	64.2	147	60.6	76.9
Danio rerio (zebrafish)	NP997977	788	46.0	64.2	146	55.6	75.6
Anas platyrhynchos (mallard)	ACS92628	783	39.7	58.0	145	58.1	75.0
Gallus gallus (chicken)	AEX25757	793	39.0	56.2	145	56.2	73.8
Homo sapiens (human)	AAY85648	784	39.0	56.5	146	58.0	73.5
Mus musculus (mouse)	AAH14693	784	38.4	56.2	146	56.2	75.0
Sus scrofa (pig)	ACZ82293	785	38.0	55.1	145	54.9	73.5
Bos taurus (Bovine)	NP776622	784	38.0	55.2	145	57.4	73.5
Xenopus tropicalis (frog)	ENSXETP00000003822	777	37.4	55.8	145	56.2	75.6
Ciona intestinalis (sea squirt)	AB49526 (EMBL)	984	19.7	34.8	144	30.3	47.3

As depicted in the multiple sequence alignment (Fig. 4), Leucine (L) residues in LRR motifs of RbTLR2 were found to be conserved among all the species considered. In addition asparagine (N) residues and phenylalanine (F) residues identified in asparagine ladder and phenylalanine spine in TLR 2 of mouse and human are well conserved in RbTLR2 LRRs (Jin et al., 2007). Moreover, consensus amino acid sequences, identified in human TLR 2-TIR domain were also appeared in the RbTLR2-TIR domain sequence, including FW motif (residues 801-802), which was located close to the C-terminal (Xu et al., 2000). Furthermore, several amino acids, in hydrophobic core of human TLR 2 were noticed in the TIR domain of RbTLR2, sharing a greater conservation among other vertebrate species considered in the multiple sequence comparison (Xu et al., 2000). Altogether, above remarks of RbTLR2, validate it as a novel member of vertebrate counterparts of TLR 2.

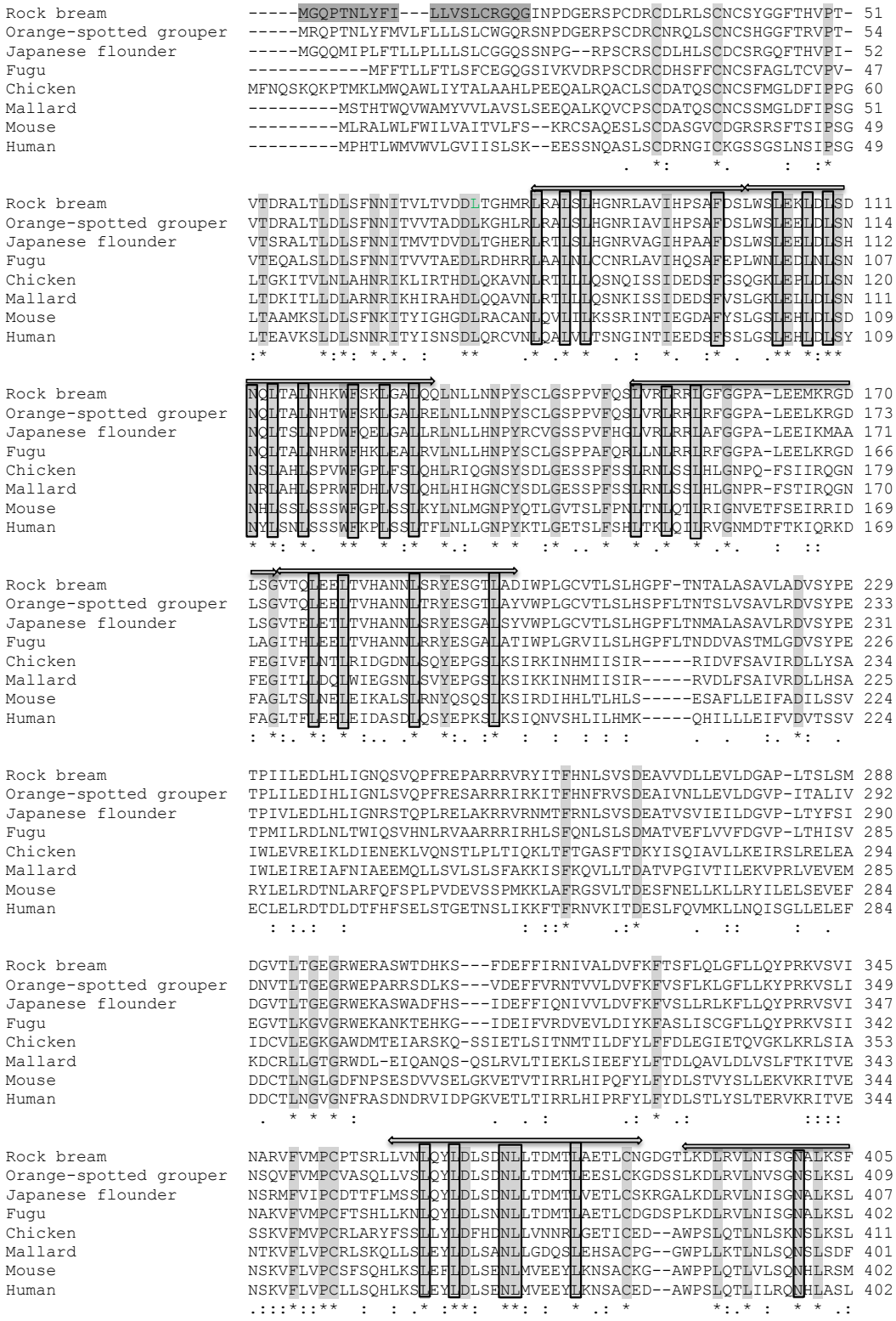

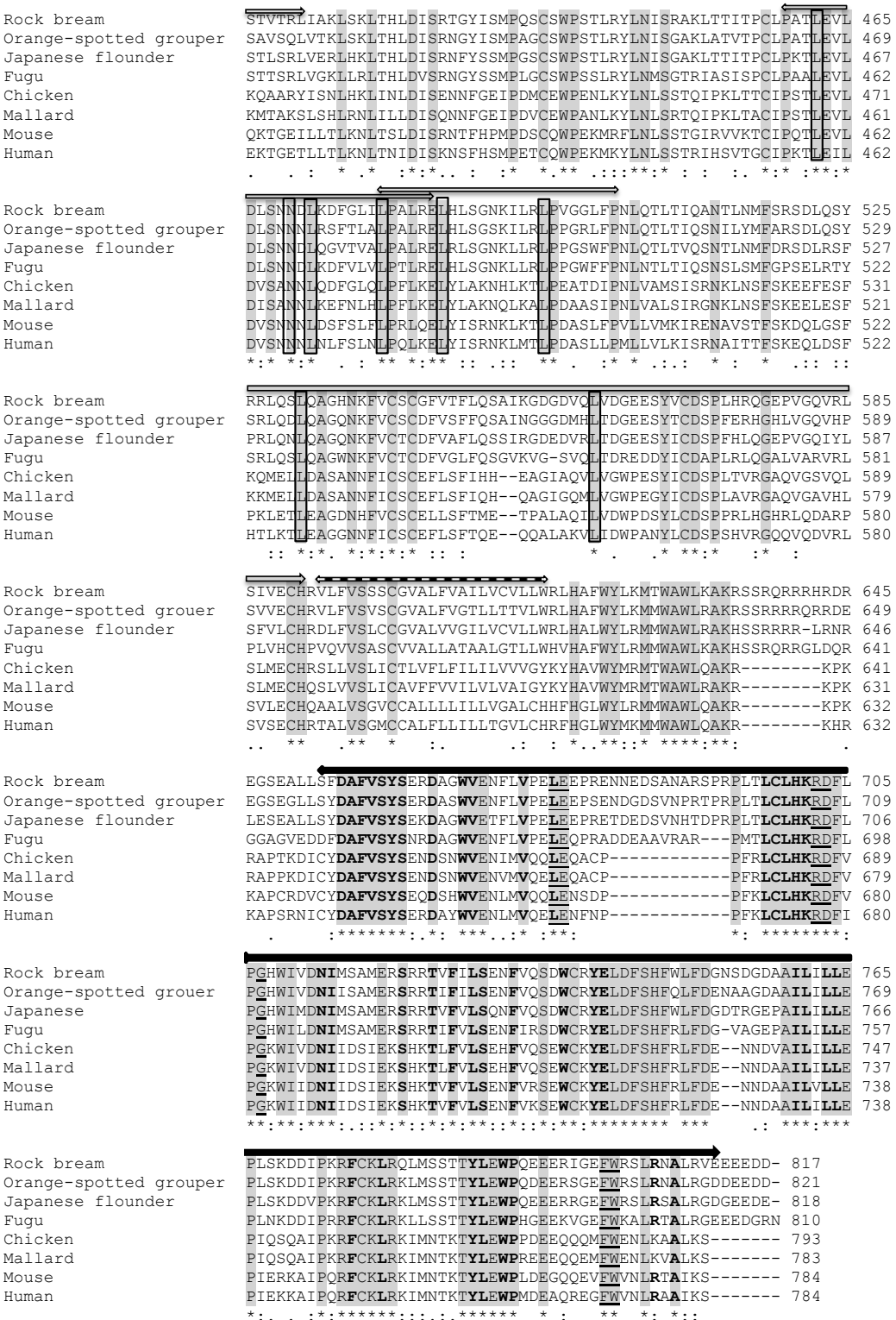

Fig. 4. Multiple sequence alignment of vertebrate TLR 2. Sequence alignments were obtained by ClustalW method. Signal peptide of RbTLR2 was indicated by dark gray shading. LRR motifs are represented by gray shaded double headed arrows, where C-terminal LRR was denoted using single head arrow. Transmembrane domain was indicated using pattern filled double headed arrow, whereas TIR domain was depicted using solid black double headed arrow. The conserved asparagine (N) residues and phenylalanine (F) residues identified in asparagine ladder and phenylalanine spine respectively along with conserved Lucien (L) residues in LRRs, were boxed. Consensus amino acid sequences, including FW motif, showing conservation and conserved residues in hydrophobic core of TIR domain, were underlined and bolded respectively.

According to the phylogenetic tree construct, RbTLR2 was clustered with its fish counterparts, altogether forming an independent clade, sub clustering with TLR 2 of orange spotted grouper, showing a fairly high bootstrap value (77) (Fig. 5). This evolutionary relationship confirms its ancestral origin of piscines. Furthermore, the tree reveals the sub grouping of corresponding mammalian and avian counterparts separately, including in the non-fish vertebrate clade. As expected, TLR 2 from sea squirt, a lower vertebrate similitude showed a distant relationship with other vertebrate counterparts, forming an out group from the main tree.

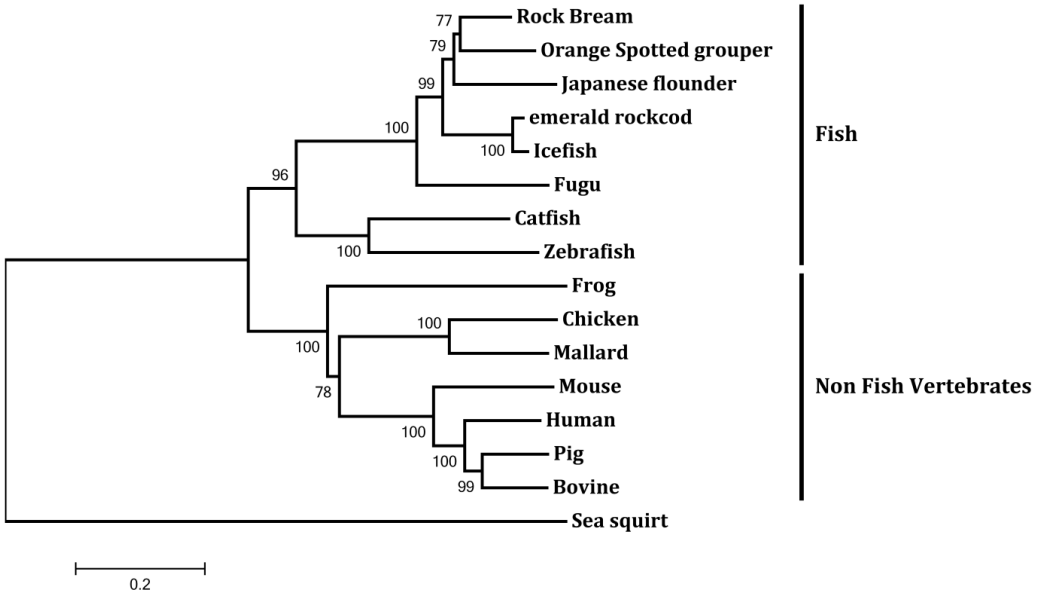

Fig. 5. Phylogenetic tree generated based on ClustalW alignment of deduced amino acid sequences of various TLR 2 protein sequences, estimated by neighbor-joining method in MEGA version 3.0. Bootstrap values are shown on the linages of the tree.

3.2. RbTLR2 genomic DNA organization

The complete RbTLR2 gDNA was 10849 bp, consisting of eleven exons interrupted by 10 introns (Fig. 6). The sequence around the exon/intron boundaries followed the AG-GT rule which is important in splicing process. Identified and characterized gDNA sequence was compared with previously elucidated TLR 2 genomic architectures of five different teleosts and two different mammalian species (Fig. 6). Regarding the genomic length, RbTLR2 was the most eminent TLR 2 variant among the teleost counterparts considered. RbTLR2 genomic organization was highly compatible with the genomic structure of TLR 2 genes of Fugu and Japanese flounder, where number of exons is identical with fugu. However, some exons and introns of RbTLR2 were relatively large, which have contributed to enhance its genome size significantly, compared to the above compatible multiexonic teleost similitudes. TLR 2 of zebrafish and catfish contain only single exon, showing an intron less organization,

which are coupling with the genome architecture of human and mouse TLR 2s, where coding region is restricted to a signal exon. This observation reinforces the notion that the TLR 1 family which includes TLR 2 as a member, demonstrates more species specific adaptations, compared to other TLR families (Roach et al., 2005). Furthermore, as an agreement with the diversity of TLR 2 gDNA arrangement in teleost species, in phylogenetic analysis, TLR 2 similitudes of fugu and flounder exhibited higher evolutionary proximity with RbTLR2 rather than catfish and zebrafish (Fig. 6). This observation convinces us an evolutionary potential of intron integration into teleost TLR 2 genes.

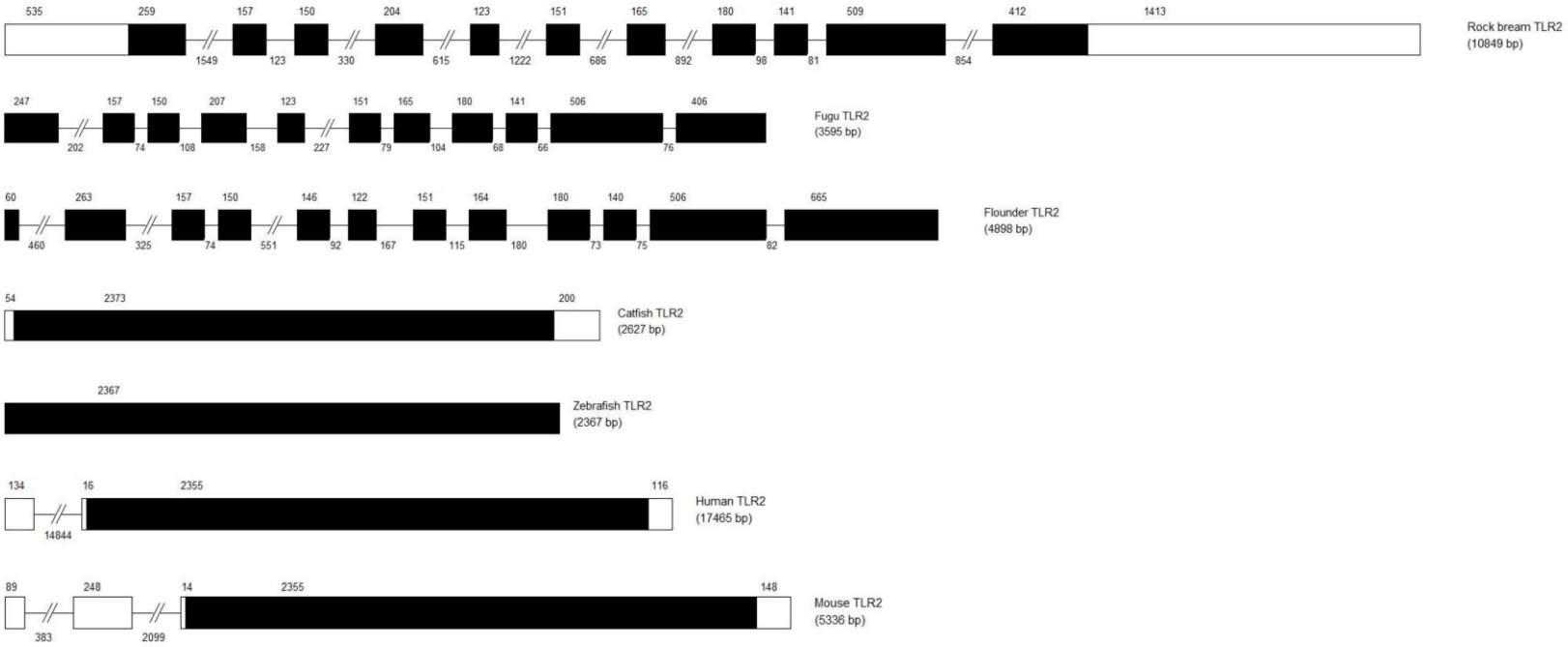

Fig. 6. Genomic organization of TLR 2 gene from different species. The exons and introns are indicated by boxes and solid lines, respectively. The sizes of exons are indicated above the exons and sizes of introns are indicated below the introns. When representing introns sequence regions larger than 100bp are truncated by two inclined lines (Sequence direction - 5' →3'). Sequence architectures of other vertebrates used in the comparison, except mouse (Gene bank accession - AC000025) were extracted from Baoprasertkul et al. (2007).

3.3. *In silico* derived RbTLR2 promoter sequence

The anticipated promoter region of RbTLR2, around 1 kb sequence, revealed the presence of several potential transcription factor binding sites (Fig. 7), including the *cis* elements that bind with transcriptional factors stimulated by immune signals generated by pathogenic infections, such as AP1, SP1 and NF-κB (Hess et al., 2004; Lacroix et al., 2002; Parrott et al., 1991; Tian and Brasier, 2003), convincing the potent role of RbTLR2 in innate immune responses. In addition, since elevated NF-κB expression can be triggered by TLR mediated signaling, including TLR 2 (Martin and Wesche, 2002), in turn involvement of NF-κB in TLR 2 transcription is reinforced, as convinced by the predicted promoter region. Moreover some of the above mentioned transcriptional factor binding sites could also be empirically detected in human TLR 2 core promoter sequence (SP1 and NF-κB), substantiating the validity of the predicted sequence (De Oliveira et al., 2011).

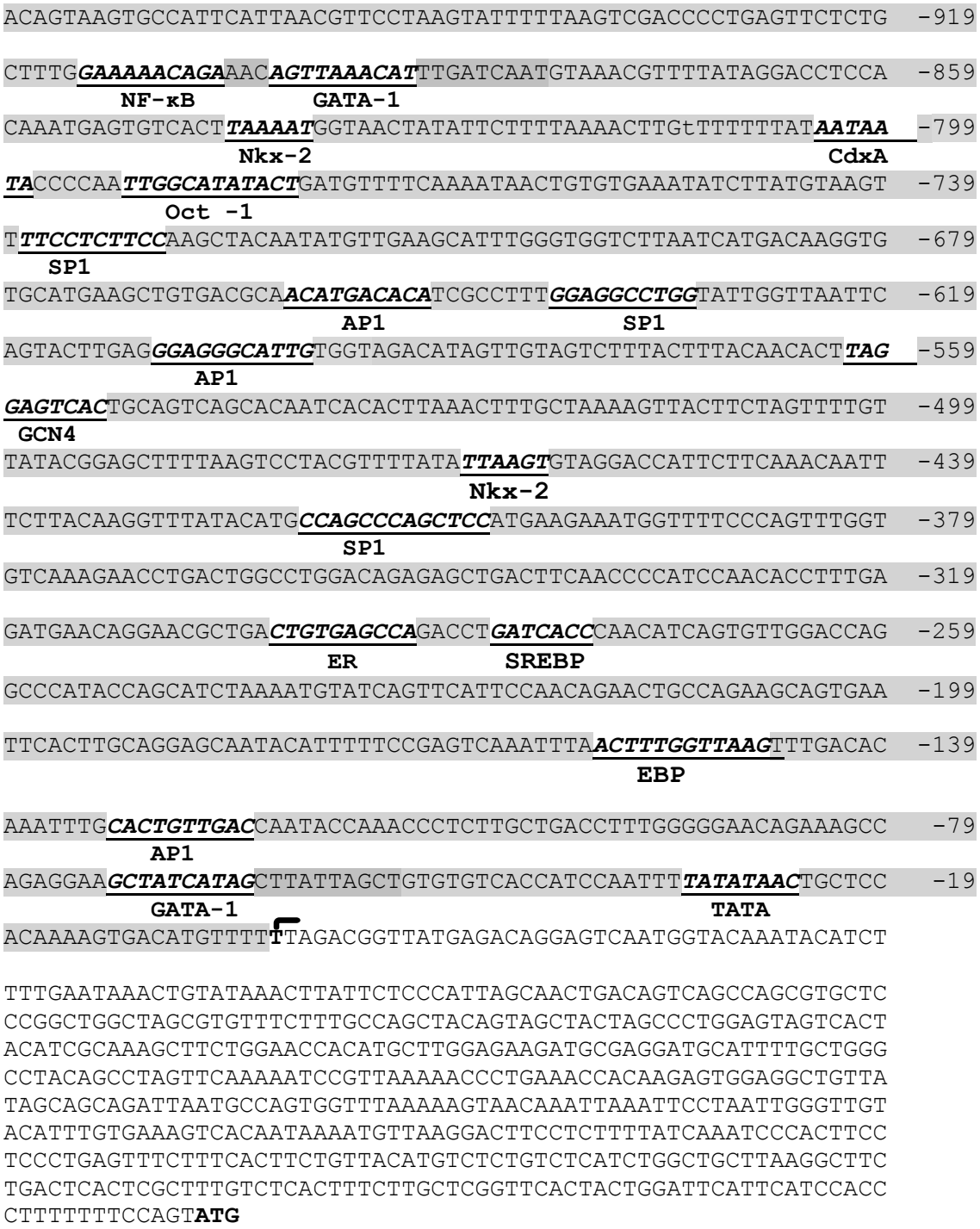

Fig. 7. Predicted promoter region of RbTLR2 with 5' UTR and start codon ATG (bold). The transcription initiation site (+1) is denoted by a curved arrow from which 5' UTR starts. Anticipated transcription factor binding sites are indicated by bolded and underlined italic letters, with their corresponding identity.

3.4.Tissue specific mRNA expression profile of RbTLR2

According to qRT-PCR carried out using different tissues of healthy fish, mentioned in section 2.6, ubiquitous expression of RbTLR2 mRNA was detected albeit in different magnitudes (Fig. 8) Greatest RbTLR2 expression was observed in spleen whereas lowest expression was detected in muscle. Liver tissue and the kidney showed moderately high TLR 2 expression in rock bream while RbTLR2 mRNA was found to be less abundant in remaining tissues. Abundant expression of RbTLR2 in immune related tissues, such as spleen and liver (Sheth and Bankey, 2001; Tarantino et al., 2011) reinforces its potent role in immune responses. Similarly, as reported previously, universally distributed pattern of TLR 2 transcription was detected in tissues of orange spotted grouper and rohu (Samanta et al., 2012; Wei et al., 2011) where strongest expression was detected in spleen in both animals, complying with our observation in rock bream. In catfish, fugu and flounder (Baoprasertkul et al., 2007; Hirono et al., 2004; Oshiumi et al., 2003) TLR 2 expression was detected in all the tissues examined , where in catfish higher transcript levels were detected in liver, brain and gill tissues whereas in flounder, peripheral blood leukocytes showed more pronounced expression. However, TLR 2 transcription analyzed in different tissues of zebrafish demonstrated a narrow distribution among the tissues, while the detectable mRNA levels were only observed in skin, brain, liver, ovary and spleen (Jault et al., 2004).

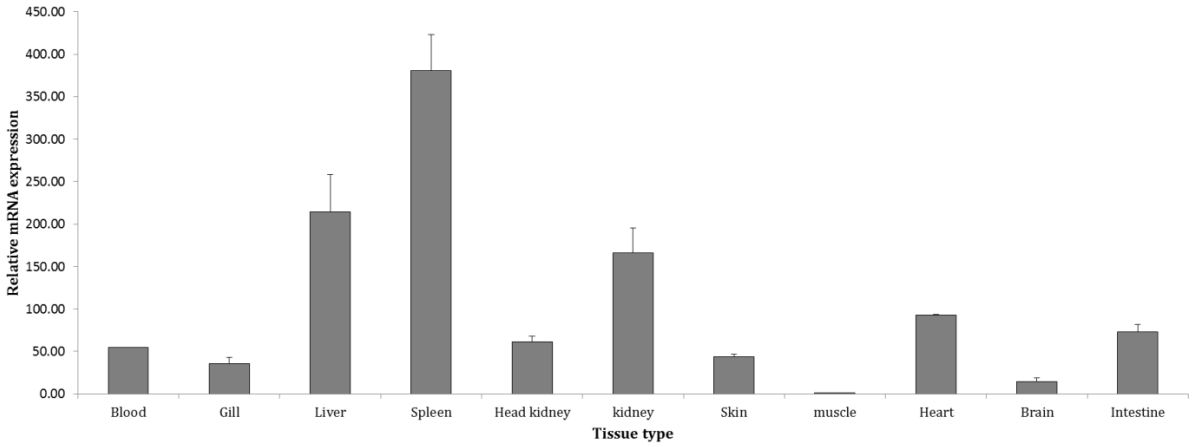

Fig. 8. The tissue specific expression analysis of RbTLR2 mRNA, determined by qRT-PCR. Expression fold changes were depicted relative to the mRNA expression level in muscle tissue. Error bars represent the SD (n=3). Expression level in every tissue was significantly different ($p < 0.05$) to each other.

3.5. RbTLR2 mRNA expression upon viral and bacterial stimulations

In order to evaluate the transcriptional response of RbTLR2 in liver tissue upon viral and bacterial stimulations along with their PAMPs, live DNA virus RBIV, which is a frequent pathogen of rock bream, poly I:C, a viral double stranded RNA (ds RNA) mimic, two live Gram positive and Gram negative bacteria, *S. iniae* and *E. tarda* respectively, and well characterized endotoxin of Gram negative bacterial cell wall, LPS were utilized. In all qRT-PCR analyses, mRNA expression levels with respect to RbTLR2 were detected relative to the corresponding rock bream β-actin expression folds and further normalizing to the corresponding PBS injected controls at each time point. Relative expression level of 0 h time point (un-injected control) was kept as the basal line.

According to the *E. tarda* challenge, at 12 h and 24 h post injection (p.i.), RbTLR2 transcript level was significantly ($p < 0.05$) up-regulated, depicting around 1.6 and 2.0

relative expression fold increase, respectively and reaching to the basal level at 48 h p.i (Fig. 9). The positive regulation observed in *E. tarda* challenge shows an agreement with previously reported transcriptional profiles of TLR 2s induced with Gram negative bacteria. Among them, in rohu, mRNA level of TLR 2 in liver was significantly ($p < 0.05$) elevated upon stimulation of same bacteria, at 12 h and 24 h p.i., showing consistent results (Samanta et al., 2012). Similarly, in some other tissues of rohu, including intestine, heart and skin, TLR 2 transcription was reported to be significantly ($p < 0.05$) increased due to *E. tarda* injection. Moreover, blue catfish TLR 2 in head kidney exhibited significant transcriptional elevations at 4 h, 24 h and 72 h p.i, following an immune challenge with *Edwardsiella ictaluri*. However a significant down regulation was also observed in blue catfish in spleen, upon the same induction at 72 h p.i. convincing a complex behavior of TLRs (Baoprasertkul et al., 2007) in antibacterial immune responses. Compliant inductions was also noticed in a previous study on TLR 2 of orange spotted grouper (Wei et al., 2011) albeit it was a comparatively prolonged challenge experiment (7 days), in which compatible transcriptional elevations of TLR 2 was detected in head kidney and spleen upon the stimulation with *Vibrio alginolyticus*, a Gram negative bacteria.

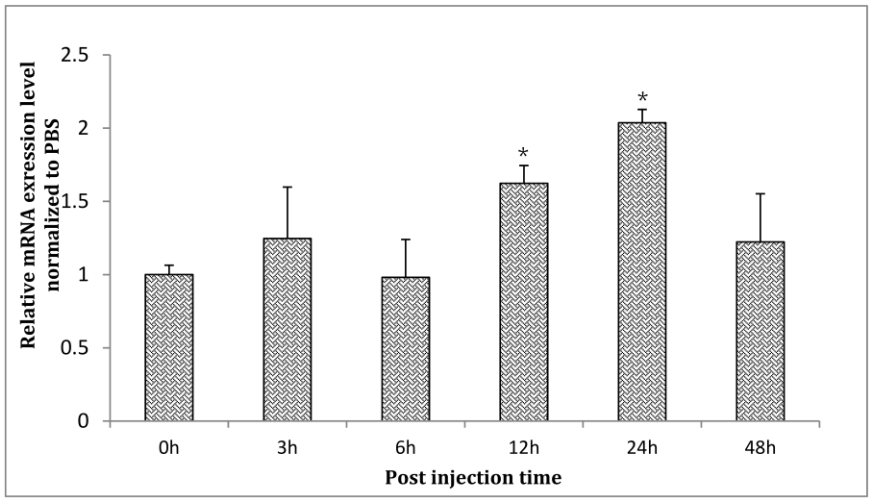

Fig. 9. Expression profile of RbTLR2 mRNA in liver tissues upon stimulation with *E. tarda* bacteria, determined by qRT-PCR. The relative expression was calculated by the $2^{-\Delta\Delta CT}$ method, using rock bream β-actin as reference gene, normalizing to the corresponding PBS injected controls at each time point. The relevant expression fold at 0 h post-injection (un-injected control) was kept as the basal line. Error bars represents the SD (n=3); *$p < 0.05$.

Upon LPS stimulation RbTLR2 mRNA expression was detected to be elevated in early phase (at 3 h p.i. and 6 h p.i.) as well as late phase (48 h p.i), significantly ($p < 0.05$), where in late phase reaching to the highest fold difference (~ 6.4 fold) (Fig. 10). This observations is compatible with TLR 2 expression profile upon LPS induction in spleen of orange spotted grouper (Wei et al., 2011), where TLR 2 was significantly ($p < 0.05$) up-regulated at 24 h p.i.

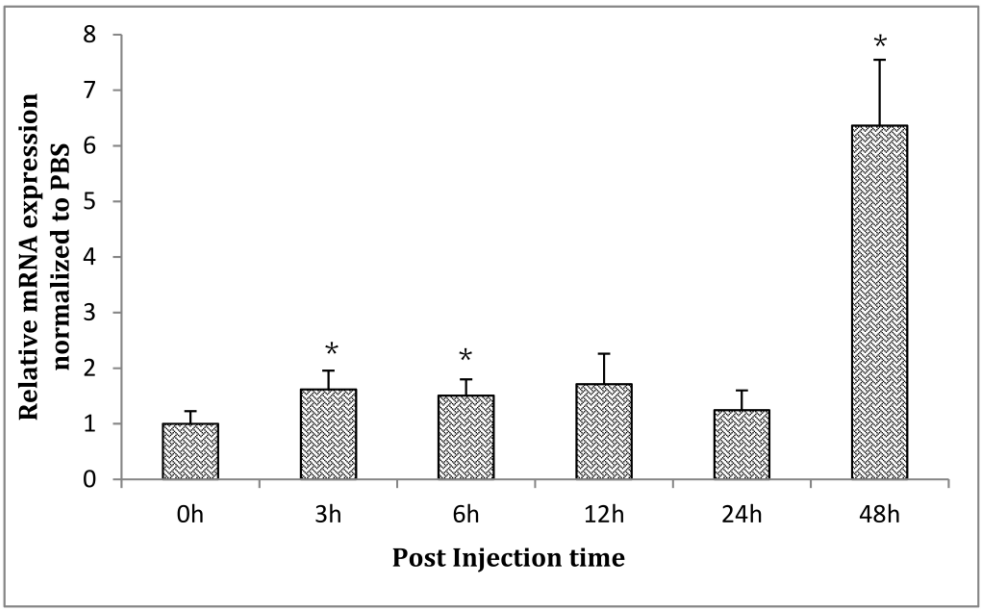

Fig. 10. Expression profile of RbTLR2 mRNA in liver tissues upon stimulation with LPS, determined by qRT-PCR. The relative expression was calculated by the $2^{-\Delta\Delta CT}$ method, using rock bream β-actin as reference gene, normalizing to the corresponding PBS injected controls at each time point. The relevant expression fold at 0 h post-injection (un-injected control) was kept as the basal line. Error bars represents the SD (n=3); *$p <$ 0.05.

Consistent with the majority of previous reports on TLR 2 agonists, RbTLR2 transcript level was significantly ($p < 0.05$) up-regulated upon *S. iniae* injection at all the time points considered where peak fold change (~ 4.0 fold) was reported at 12 h p.i. (Fig. 11), reinforcing the distinctive ability of TLR 2 to recognize PAMPs on Gram positive bacteria. Most of the teleost species also have elicited positive immune responses to inductions with Gram positive bacteria or its agonists, including transcriptional elevation observed in zebrafish, after 8 week post challenge with *Myobacterium* species (Jault et al., 2004) and up-regulations noticed in Japanese flounder upon peptidoglycan (PGN), a characteristic PAMP on Gram positive bacteria at 1 h and 3 h p.i. (Hirono et al., 2004). In addition, following the injections of prototype ligands of Gram positive bacteria, lipoteichoic acid

(LTA) and PGN, TLR 2 transcription was elevated compared to basal level in rohu peripheral blood leukocytes (PBL), at 2 h and both at 2 h and 4 h respectively. Similarly, rohu TLR 2 transcript levels were found to be boosted by live Gram positive bacteria, *Streptococcus ubers* in liver tissue at 12 h and 24 h p.i. Furthermore similar transcriptional modulations were commonly observed in kidney, intestine and skin at 24 h, 12 h and both 12 h alone with 24 h p.i., respectively in rohu.

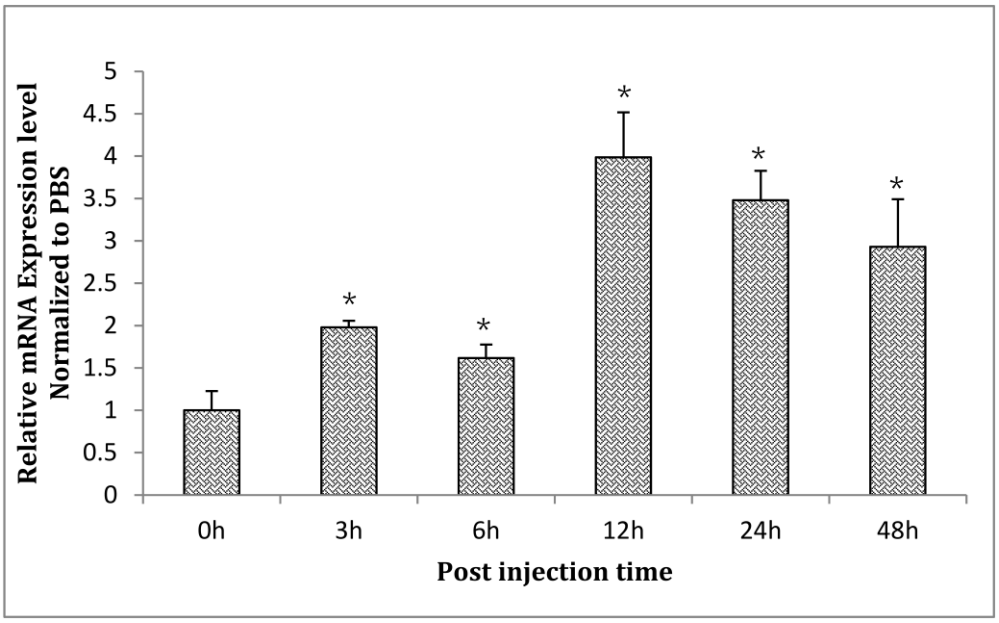

Fig. 11. Expression profile of RbTLR2 mRNA in liver tissues upon stimulation with *S. iniae* bacteria, determined by qRT-PCR. The relative expression was calculated by the $2^{-\Delta\Delta CT}$ method, using rock bream β-actin as reference gene, normalizing to the corresponding PBS injected controls at each time point. The relevant expression fold at 0 h post-injection (un-injected control) was kept as the basal line. Error bars represents the SD (n=3); *$p < 0.05$.

Revealing the potency of retroviral genome to induce immune responses via TLR 2 mediated signaling pathway in rock bream, RbTLR2 was significantly ($p < 0.05$) induced upon Poly I:C injection from 12 h p.i onwards at each time point (Fig. 12), complying with

the detected transcriptional up-regulations in Japanese flounder at 3 h and 6 h p.i. with Poly I:C in PBLs (Hirono et al., 2004). Furthermore in that report, TLR 2 expression was correlated with a previously experienced induction of interferon inducible antiviral protein Mx, which is a downstream molecule in toll signaling pathway. Moreover, above observations are further consistent with the significant ($p < 0.05$) elevations observed in orange spotted grouper upon the same stimulant, where both in head kidney and spleen demonstrated augmented transcript level at 24 h p.i. compared to the basal (Wei et al., 2011) . However, clear strategy of recognizing genomic constituents of viral infections by TLR 2 in teleosts is yet to be discovered, since viral genome cannot be exposed to the cell membrane receptors like TLR 2 before the internalization of the particular virus into host cells, according to the existent knowledge, unless otherwise viral particles are processed by a primary mechanism.

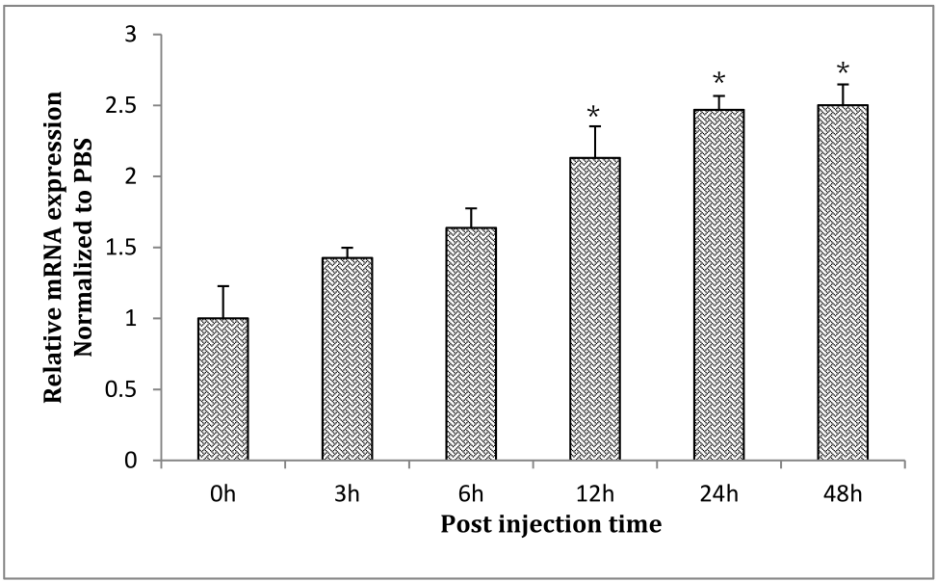

Fig. 12. Expression profile of RbTLR2 mRNA in liver tissues upon stimulation with Poly I:C, determined by qRT-PCR. The relative expression was calculated by the $2^{-\Delta\Delta CT}$ method, using rock bream β-actin as reference gene, normalizing to the corresponding PBS injected controls at each time point. The relevant expression fold at 0 h post-injection

(un-injected control) was kept as the basal line. Error bars represents the SD (n=3); *p < 0.05.

As a novel finding in teleost species, RbTLR2 transcript level was raised significantly (p < 0.05) by immune stimulation using DNA virus, RBIV, at 12 h p.i and 48 h p.i reflecting the potential involvement of RbTLR2 in antiviral immune responses (Fig. 13). This suggestion can be substantiated by the fact that TLR 2 actively involves in mammalian host defense upon viral infections, especially due to DNA viruses, where TLR 2 recognizes external viral components such as envelope glycol proteins (Xagorari and Chlichlia, 2008), as toll signaling was found to be more or less similar between mammals and teleosts (Bricknell and Dalmo, 2005). However, according to the graph (Fig. 13), at 24 h p.i TLR 2 expression was again reached to the basal level after the elevation at 12 h p.i., before the subsequent elevation, which marked the most eminent fold difference (~3.2 fold) among each time point. Similar pattern of TLR 2 expression was also reported in head kidney of Japanese flounder upon VHSV induction, where between 6 h p.i and 4 day p.i. at three time points, mRNA expression was under-expressed (Avunje et al., 2011), along with the higher viral load in the tissue, which may be attributed with the evasion mechanisms of the virus. Nevertheless, subsequently, the increased level of viral particles could be compensated by eliciting a stronger immune response, reflecting through over-expressed TLR 2 with higher fold difference. Also, same explanation can be applied to the referred observation on RbTLR2 transcriptional pattern, until the performance of further investigations.

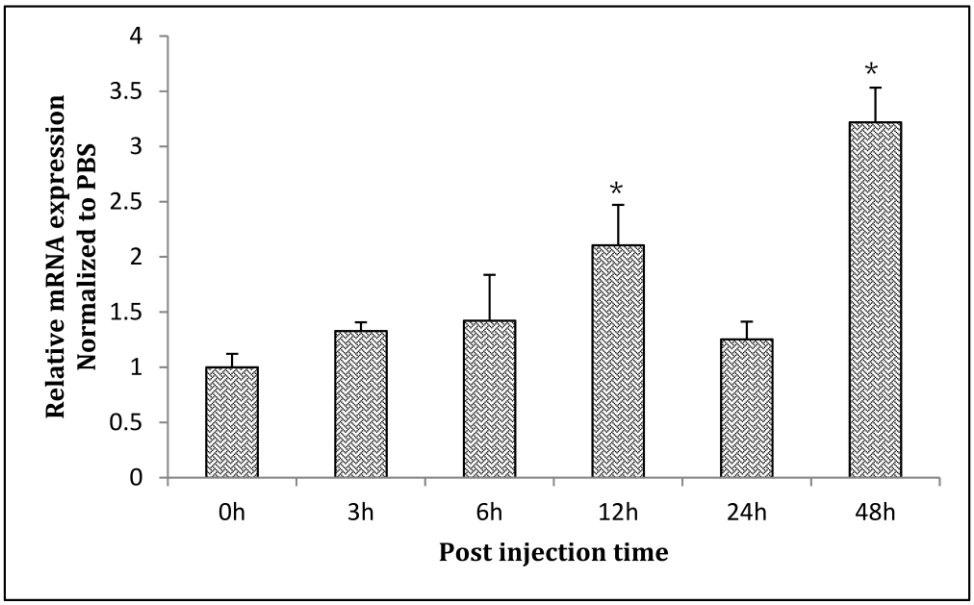

Fig. 13. Expression profile of RbTLR2 mRNA in liver tissues upon stimulation with RBIV, determined by qRT-PCR. The relative expression was calculated by the $2^{-\Delta\Delta CT}$ method, using rock bream β-actin as reference gene, normalizing to the corresponding PBS injected controls at each time point. The relevant expression fold at 0 h post-injection (un-injected control) was kept as the basal line. Error bars represents the SD (n=3); *p < 0.05.

According to the overall insight of transcriptional modulation upon five different immune stimulants, as described above, we can speculate that RbTLR2 is a potent mediator of antibacterial and antiviral host defense, further reinforcing the previous revelations on LPS and retroviral (dsRNA) genome as potential agonists of TLR 2 in teleosts. However, further research studies have to be performed, in order to reveal the overall defensive role of RbTLR2, while analyzing the complete signaling pathways initiated by RbTLR2, since the downstream molecules and respective inducible cytokines are yet to be identified from rock bream.

Chapter II

Caspase 3 from rock bream (*Oplegnathus fasciatus*): Genomic characterization and transcriptional profiling upon bacterial and viral inductions

1. ABSTRACT

Caspase 3 is a prominent mediator of apoptosis and participates in the cell death signaling cascade. In this study, caspase 3 was identified (Rbcasp3) and characterized from rock bream (*Oplegnathus fasciatus*). The full-length cDNA of Rbcasp3 is 2683 bp and contains an open reading frame of 849 bp, which encodes a 283 amino acid protein with a calculated molecular mass of 31.2 kDa and isoelectric point of 6.31. The amino acid sequence resembles the conventional caspase 3 domain architecture, including crucial amino acid residues in the catalytic site and binding pocket. The genomic length of Rbcasp3 is 7529 bp, and encompasses six exons interrupted by five introns. Phylogenetic analysis affirmed that Rbcasp3 represents a complex group in fish that has been shaped by gene duplication and diversification. Many putative transcription factor binding sites were identified in the predicted promoter region of Rbcasp3 including immune factor- and cancer signal-inducible sites. Rbcasp3, excluding the pro-domain, was expressed in *Escherichia coli.* The recombinant protein showed a detectable activity against the mammalian caspase 3/7-specific substrate DEVD-*p*NA indicating a functional role in physiology. Quantitative real time PCR assay detected Rbcasp3 expression in all examined tissues, but with high abundance in blood, liver and brain. Transcriptional profiling of rock bream liver tissue revealed that challenge with lipopolysaccharides (LPS) caused prolonged up-regulation of Rbcasp3 mRNA whereas, *Edwardsiella tarda* (*E.tarda*) stimulated a late-phase significant transcriptional response. Rock bream iridovirus (RBIV)

up-regulated Rbcasp3 transcription significantly at late-phase, however polyinosinic-polycytidylic acid (poly I:C) induced Rbcasp3 significantly at early-phase. Our findings suggest that Rbcasp3 functions as a cysteine-aspartate-specific protease and contributes to immune responses against bacterial and viral infections.

2. MATERIALS AND METHODS

2.1 Identification of full-length cDNA sequence of Rbcasp3

Using the Basic Local Alignment Tool (BLAST) algorithm (http://www.ncbi.nlm.nih.gov/BLAST), full-length cDNA sequence of caspase 3 (contig number-07658) in -rock bream was identified from a previously established cDNA sequence data base, based upon data from a next generation DNA sequencing technology, the GS-FLX titanium system (DNA Link, Republic of Korea).

2.2. Rbcasp3 genomic BAC library construction and PCR screening.

Using rock bream genomic DNA, a random sheared bacterial artificial chromosome (BAC) library was custom constructed (Lucigen, USA). The library was screened by PCR in order to identify the clone containing the full-length Rbcasp3 gene using a sequence specific primer pair Rbcasp3-qF and Rbcasp3-qR (Table 3), designed according to the identified Rbcasp3 cDNA sequence, as described in Chapter I, section 2.2. The identified BAC clone was sequenced by GS-FLX^{TM} system (Life Sciences, USA).

2.3. *In silico* analysis of rock bream caspase 3 DNA and protein sequences

The orthologous sequences of Rbcasp3 were compared by the BLAST search program. Pairwise sequence alignment (http://www.Ebi.ac.uk/Tools/emboss/align) and multiple sequence alignment (http://www.Ebi.ac.uk/Tools/clustalw2) were performed using the EMBOSS needle and ClustalW2 programs, respectively. The phylogenetic relationship of Rbcasp3 was determined using the Neighbor-Joining method and Molecular Evolutionary Genetics Analysis (MEGA) software version 4 (Tamura et al, 2007). Prediction of protein domains was carried out using the ExPASy-prosite data base (http://prosite.expasy.org) and the MotifScan scanning algorithm (http://myhits.isb-sib.ch/cgi-bin/motif_scan). Some

properties of Rbcasp3 were determined by ExPASy Prot-Param tool (http://web.expasy.org/protparam).

Genomic sequence of Rbcasp3 obtained from the BAC clone was used to identify the exon-intron structure and predict the promoter region along with potential transcriptional factor binding sites. The transcription initiation site (TIS) was predicted using the online neural network promoter prediction tool from Berkeley Drosophila Genome Project (Reese, 2001). Potential cis acting elements located ~1Kb upstream of the TIS were detected using TFSEARCH ver.1.3 and Alibaba 2.1 software. Furthermore, the tertiary structure of Rbcasp3 pro-enzyme was modeled based on the ab-initio protein prediction strategy, using the online server I-TASSER (Roy et al, 2010; Zhang, 2008). Subsequently, the three dimensional (3D) image was generated utilizing RasMol 2.7.5.2 software.

2.4 Expression and purification of recombinant Rbcasp3 (rRbcasp3)

Recombinant Rbcasp3, excluding the pro-domain, was expressed as a fusion protein with Maltose Binding Protein (MBP) and purified as described previously with some modifications (Umasuthan et al, 2011). Briefly, the Rbcasp3 gene encoding residues 33-283 was amplified using the sequence specific primers Rbcasp3-F and Rbcasp3-R with restriction enzyme sites for *Eco*RI and *Pst*I respectively (Table 1). The PCR was performed in a TaKaRa thermal cycler in a total volume of 50 µL with 5 U of Ex*Taq* polymerase (TaKaRa, Japan), 5 µL of 10x Ex *Taq* buffer, 8 µL of 2.5 mM dNTPs, 80 ng of template, and 20 pmol of each primer. The reaction was carried out at 94 °C for 30 sec, 55 °C for 30 sec, 72 °C for 1min and final extension at 72 °C for 5 min. The PCR product (~ 753 bp) was resolved on a 1% agarose gel, excised and purified using the AccuprepTM gel purification kit (Bioneer Co. Korea). The digested pMAL-c2X vector (35 ng) and PCR product (15 ng) were ligated using Mighty Mix (7.5 µl; TaKaRa) at 4 °C overnight. The

ligated pMAL-c2X/Rbcasp3 product was transformed into DH5α cells and sequenced. Sequence confirmed recombinant expression plasmid was transformed into *Escherichia coli* BL21 (DE3) competent cells. The recombinant Rbcasp3 protein was overexpressed using isopropyl-β-galactopyranoside (IPTG, 1 mM final concentration) at 37 °C for 3 h, after which the protein was purified using pMAL protein fusion and purification system (New England Biolabs, USA).The purified protein was eluted with elution buffer (10 mM maltose) and the concentration was determined by the Bradford method using bovine serum albumin (BSA) as the standard (Bradford, 1976). The Rbcasp 3 samples collected from different purification steps were analyzed on 12% SDS-PAGE under reduced conditions, with standard protein size marker (TaKaRa - Japan). The gel was stained with 0.05% Comassie blue R-250, followed by a standard de-staining procedure.

2.5 Hydrolyzing activity assay of rRbcasp3

With the objective of characterizing the purified rRbcasp3, hydrolyzing activity was analyzed by using caspase 3 activity assay kit (BioVision, USA) following manufacturer's protocol. Briefly, the purified protein was adjusted to 2 µg/µL and 50 µL was mixed with 50 µL 2x reaction buffer and 5 µL of 4 mM caspase 3/7 specific substrate (DEVD-*p*NA), followed by incubation at 37 °C for 2 h. The cleavage and release of *p*NA was measured by monitoring absorbance at 400 nm using a spectrophotometer. In order to assess the specificity of Rbcasp 3 against DEVD-*p*NA, its activity against caspases 9 and caspases 8 substrates (LEHD-*p*NA and IETD-*p*NA, respectively from Bio Vision USA) was also analyzed. Each assay was conducted with the MBP control, to determine the effect of fusion protein on the activity of rRbcasp3. All the assays were carried out with three replicates. The mean absorbance values obtained in the assay for both fusion protein and MBP alone were expressed to represent the hydrolyzing activities.

2.6 Experimental fish and tissue collection

Animal rearing was performed as described in the chapter I, section 2.4. All individuals were allowed to acclimate for one week prior to experimentation. Whole blood (1 mL/ fish) was collected from the caudal fin using a sterilized syringe, and the sample was immediately centrifuged at 3,000 x g for 10 min at 4 °C to separate the blood cells from the plasma. The collected cells were snap-frozen in liquid nitrogen. Meanwhile, the sampled fish was sacrificed and the gill, liver, skin, spleen, head kidney, kidney, skin, muscle, brain and intestine were excised and immediately snap-frozen in liquid nitrogen and stored at -80 °C until use for total RNA extraction.

2.7 Immune challenge experiments

In order to determine the immune responses of Rbcasp3, *E. tarda*, RBIV, LPS and the viral dsRNA mimic poly I:C were employed as immune-stimulants in time course experiments. Tissues were collected as described in section 2.6. The immune challenge experiments were carried out as described in Chapter I, section 2.5. At least three animals for the tissue collection from each challenge group at each time point.

2.8 Total RNA extraction and cDNA synthesis

Total RNA was extracted from each of the excised tissues by using the Tri Reagent^{TM} (Sigma-Aldrich, USA). Concentration of RNA was determined at 260 nm in a UV-spectrophotometer (Bio-Rad, USA) and diluted to 1 µg/µL. 2.5 µg of RNA from selected tissues was applied in cDNA synthesis using cDNA synthesis kit (TaKaRa, Japan) according to the manufacturer's instructions. Finally, the newly synthesized cDNA was diluted 40-fold (total 800 µl) and stored at -20°C until needed for further analysis.

2.9 Rbcasp3 mRNA expression analysis by quantitative real time reverse transcription (qRT- PCR)

qRT-PCR was used to detect the expression levels of Rbcasp3 in blood, gill, liver, spleen, head kidney, kidney, skin, muscle, brain and intestine tissues, and the temporal expression of Rbcasp3 in liver. Total RNA was extracted at different time points following immune challenge, and the first-strand cDNA synthesis was carried out as described in section 2.8. qRT-PCR was carried out using the thermal cycler Dice^{TM} Real Time System (TP800; TaKaRa, Japan) in a 15 µL reaction volume containing 4 µl of diluted cDNA from each tissue, 10 µL of 2x TaKaRa Ex Taq^{TM}, SYBR premix, 0.5 µL of each primer (Rbcasp3-qF and Rbcasp3-qR; Table-3), and 5 µL of ddH_2O. The qRT-PCR was performed under the following conditions: 95 °C for 10 sec, followed by 35 cycles of 95 °C for 5 sec, 58 °C for 10 sec and 72 °C for 20 sec and a final cycle of 95 °C for 15 sec, 60 °C for 30 sec and 95 °C for 15 sec. The base line was set automatically by Dice^{TM} Real Time System software (version 2.00). Rbcasp3 expression was determined by the Livak ($2^{-\Delta\Delta CT}$) method (Livak and Schmittgen et al, 2001). The same qRT-PCR cycle profile was used for the internal control gene, rock bream β-actin (Genbank ID: FJ975146). All data are presented as means ± standard deviation (SD) of relative mRNA expression of three replicates. To determine statistical significance ($P < 0.05$) between the experimental and control groups, the two-tailed paired *t*-test was carried out.

Table 3. Primers used in the study on Rbcasp3. F and R refer to forward and reverse primers, respectively. The lowercase letters indicate restriction enzyme sites introduced for cloning.

Name	Purpose	Sequence (5'→3')
Rbcasp3-F	ORF amplification (without pro- domain)	GAGAGAgaattcGCCAAGCCCAGCTCCCACAG
Rbcasp3-R	ORF amplification (without pro-domain)	GAGAGActgcagTCAAGGAGAAAAATACATCTCTTTGGTCAGCATTG
Rbcasp3-qF	qRT-PCR primer	TGAGGGTGTGTTCTTTGGTACGGA
Rbcasp3-qR	qRT-PCR primer	TTCCCACTAGTGACTTGCAGCGAT
Rb-β-actin-F	qRT PCR internal reference	TCATCACCATCGGCAATGAGAGGT
Rb-β-actin-R	qRT PCR internal reference	TGATGCTGTTGTAGGTGGTCTCGT

RESULTS

3.1 Molecular characterization and phylogenetic analysis of Rbcasp3

The full-length sequence of Rbcasp3 consists of 2756 nucleotides (nt), which is comprised of a 849 bp open reading frame (ORF) encoding 283 amino acids, a 159 bp 5' untranslated region (5' -UTR), and a 1748 bp 3' -UTR. The 3' -UTR contains a polyadenylation signal (^{2730}AATAAA^{2735}) and three RNA instability motifs (^{2027}ATTTA^{2031}, ^{2205}ATTTA^{2209}, ^{2592}ATTTA^{2596}) (Fig. 14). Moreover, the predicted molecular mass of Rbcasp3 was around 31.2 kDa and the theoretical isoelectric point was 6.31.

Fig. 14. Nucleotide and deduced amino acid sequence of Rbcasp3. The start codon (ATG), the stop codon (TGA), and the polyadenylation signal sequence (ATTAAA) are indicated by gray shading. The protein binding domain (GSWFI) and the penta-peptide

active site motif (QACRG) are depicted in boxes. Three RNA instability motifs (ATTTA) are shown by underling.

Resembling the typical caspase domain architecture, Rbcasp3 contained a putative pro-domain (residues 1-36), a large subunit (residues 52-176), and a small subunit (residues 189-283) as predicted by ExPASy Prosite server. Several amino acid residues that are known to be critical for the function of caspase 3 catalytic center (Cys^{172}, His^{130}, Gly^{131}) and binding pocket (Gln^{170}, Arg^{244}, Ser^{257}) were found to be well conserved in Rbcasp3 (Li et al, 2011). Moreover, the characteristic active site penta-peptide motif (^{170}QACRG^{174}) was also identified in the large subunit of Rbcasp3. The protein binding domain ^{218}GSWFI^{222} (Johnson and Bridgham, 2000) present within the small subunit also exhibited a significant conservation among the species analyzed with only a conservative substitution in the last amino acid of the motif for Atlantic salmon, large yellow croaker, and fugu (*Takifugu rubripes*) (Fig. 15). Similarly, the integrin recognition motif (^{152}RGD^{154}) (Pierschbacher and Rouslahti, 1984) in Rbcasp3 near the active site was found to be conserved in all species analyzed, with the exceptions of sea bass caspases 3 and medaka caspases 3A variant, wherein the aspartate residue is replaced by an asparagine in sea bass and arginine and aspartate residues are replaced by lysine and arginine residues respectively in medaka. (Fig. 15).

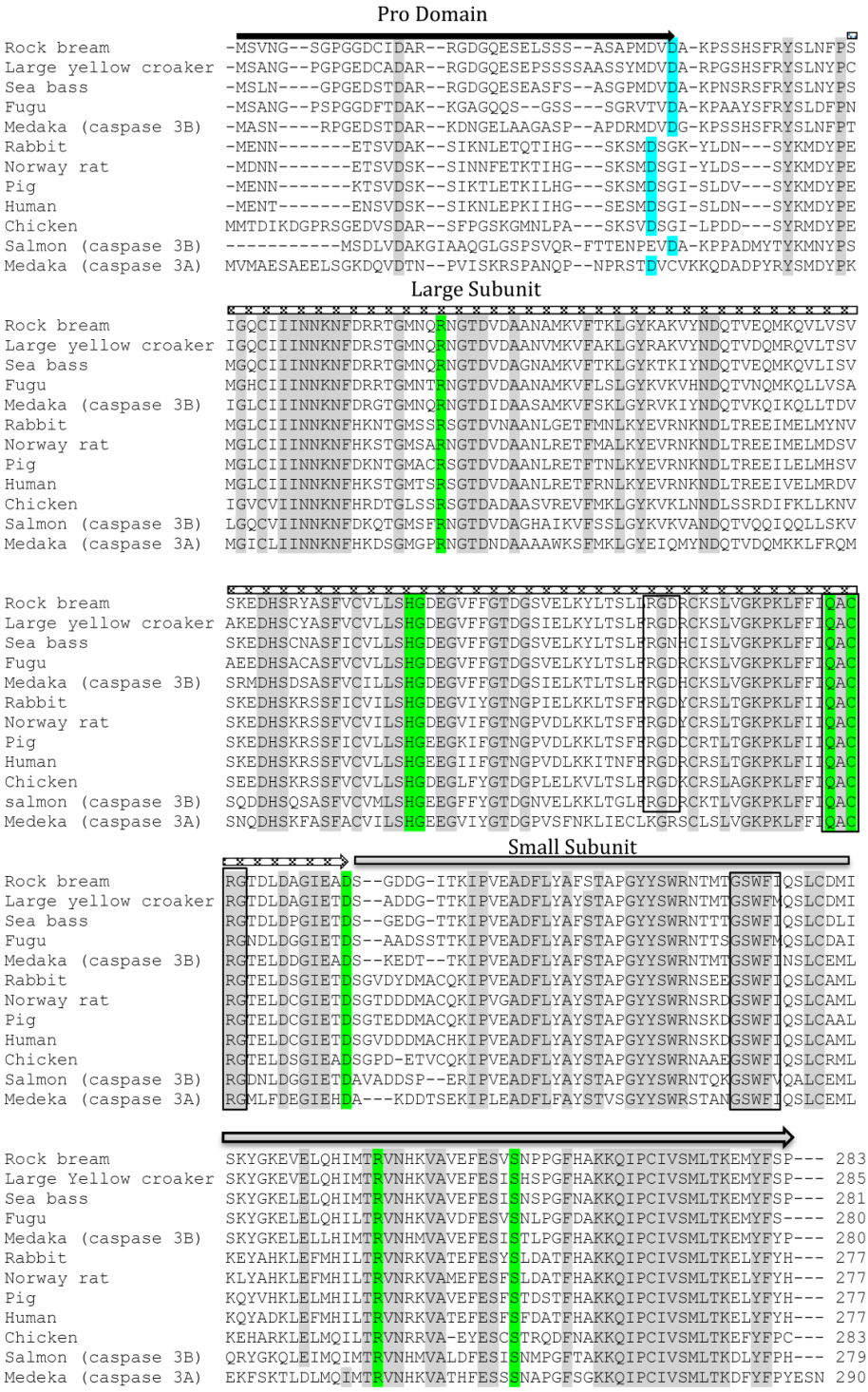

Fig. 15. Multiple sequence alignment of vertebrate caspase 3. Sequence alignments were obtained by the ClustalW method. Conserved residues are shaded in gray. The putative cleavage sites at aspartic acid residues, where the separation of relevant domains occurs, are indicated by pale blue shading. Several critical residues in the caspase 3 catalytic center and binding pocket are indicated by pale green shading. The protein

binding domain (GSWFI), the integrin recognition motif (RGD), and the penta-peptide active site motif (QACRG) are indicated by boxes.

Pairwise sequence alignment revealed that Rbcasp3 has significant identity with vertebrate orthologs; for instance, caspase 3 homologues in large yellow croaker and human shared 88.8% and 54.1% of identity with Rbcasp3, respectively. In contrast, Rbcasp3 from invertebrates showed lower identity; for example, that of black tiger shrimp shared only ~28% identity with Rbcasp3 (Table 4).

Table 4. Percent identities of Rbcasp3 gene with caspase 3 genes from other species

Common name	protein	Accession number	Identity (%)
Large yellow croaker	caspase-3	ACJ65025	88.8
European seabass	caspase-3	ABC70996	88.0
Fugu rubripes	caspase-3	AAM43816	80.3
Atlantic salmon	caspase-3 precursor	ACN11423	79.9
Japanese medaka	caspase 3B	NP001098168	78.3
Zebrafish	caspase-3	CAX14649	73.0
White cloud mountain minnow	caspase 3	ACV31395	72.8
Atlantic salmon	caspase3	NP001133393	62.8
Northern pike	caspase-3 precursor	ACO13502	61.7
Chicken	caspase-3	AAC32602	59.2
Rabbit	caspase-3 precursor	NP001075586	57.0
Pig	caspase-3 precursor	NP999296277	56.7
Norway rat	caspase-3	NP037054	55.4
Human	caspase-3 preproprotein	NP116786	54.1
House mouse	caspase3	NP033940, XP996914	53.8
African clawed frog	caspase-3 -precursor	NP001081226	52.0
Blood fluke	caspase 3	ACU88129	34.7
Southern house mosquito	caspase 3	XP001850595	32.7
Fruit fly	death executioner caspase related to Apopain	AAF55329	30.0
Black tiger shrimp	caspase 3	ADV17345	28.4

Phylogenetic analysis was carried out using the Neighbor-Joining method to compare Rbcasp3 sequence with different vertebrate and invertebrate caspase 3 members (Fig. 16). The tree revealed that Rbcasp3 forms a clade with the caspase 3 of large yellow croaker, exhibiting a fairly high bootstrap supporting value (74). Moreover, this analysis confirmed that Rbcasp3 originated from a common ancestor of vertebrates, as indicated by the clustering pattern of mammals, avians and amphibians in their relevant clades. However caspases 3A from Japanese medaka formed an out group with the other clustered fish species, showing a distant relationship with other caspases 3 counterparts from fish, considered in the analysis.

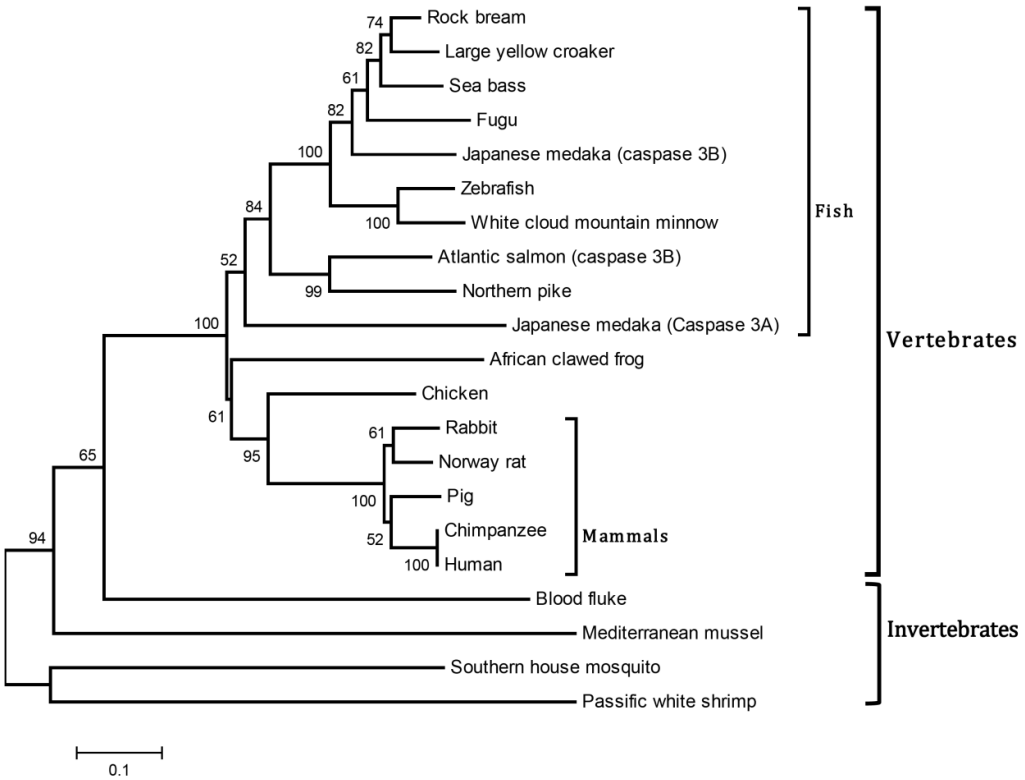

Fig. 16. Phylogenetic analysis of Rbcasp3. The tree constructed based on ClustalW alignment of deduced amino acid sequences of various caspase 3 proteins, estimated by the Neighbor-Joining method in MEGA version 4.0. Bootstrap values are shown for each

of the lineages of the tree, and major taxonomic clusters are indicated within parentheses. NCBI-GenBank accession numbers of the species used in the diagram was mentioned in Table 1.

3.2 Genomic structure and promoter analysis of Rbcasp3

The full-length Rbcasp3 gDNA is 7529 bp in length and consists of six exons interrupted by five introns. (GenBank ID: JQ315116; Fig. 17). The sequence around the exon/intron boundaries follows the AG-GT rule, which is generally important in splicing processes. The characterized gDNA sequence was compared with four previously characterized gDNA sequences of fish and human (obtained from the Ensemble genome site, (www.ensembl.org) (Fig. 17). According to the comparison, Rbcasp3 gene and caspase 3 from sea bass (Reis et al, 2007) and fugu (Ensemble ID: SINFRUT00000160403) have similar patterns of exon–intron organization, whereas the size of their introns varies considerably. The human caspase 3 gene (Ensemble ID: ENSDART00000005593) contains relatively long exons, as compared to caspase 3 in the other four organisms examined. However the characteristic common feature that is present in all five caspase 3 genes is the intron-interruption of the penta-peptide active site motif (QACRG) after its first amino acid.

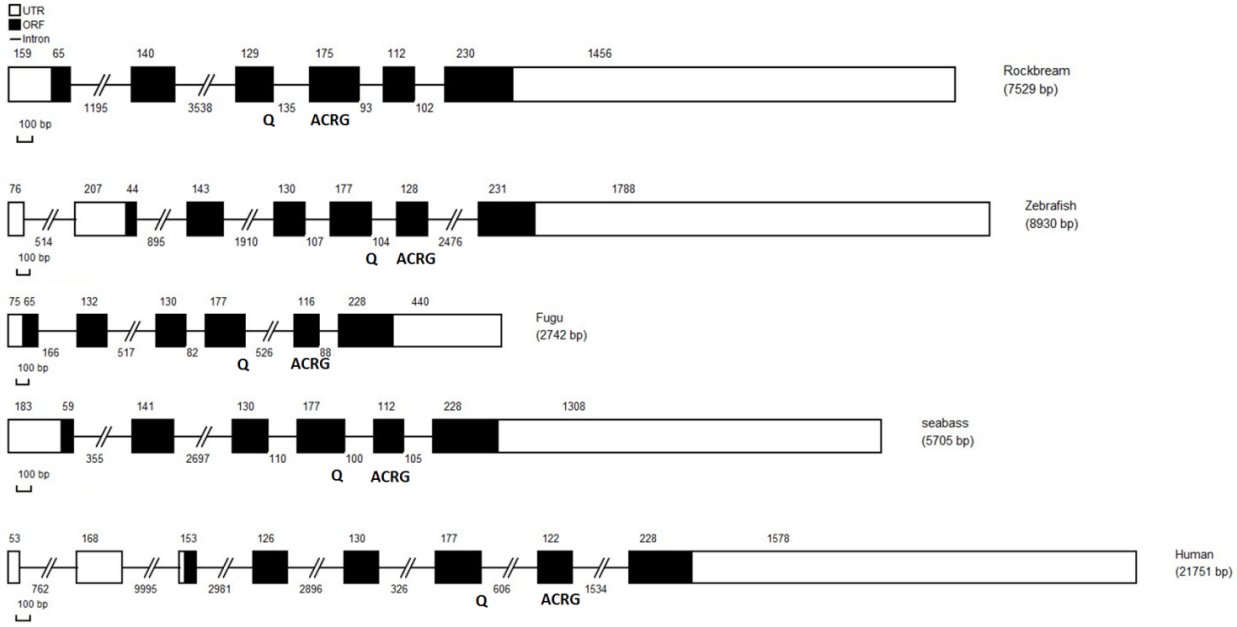

Fig. 17. **Genomic organization of the caspase 3 genes from rock bream, zebrafish, Fugu, sea bass and human**. The exons are represented by boxes and introns by solid lines. The sizes of exons are indicted above the exons and sizes of introns are indicated below the introns. Sequence regions larger than 300bp are truncated by two inclined lines (Sequence direction - 5' →3').

The sequence upstream of the Rbcasp3 transcription initiation site was analyzed and results revealed a number of potential *cis* elements, most of them are similar to those identified from previous promoter studies of other caspase 3 homologues (Liedtke et al, 2003; Liu et al, 2002) (Fig. 18).

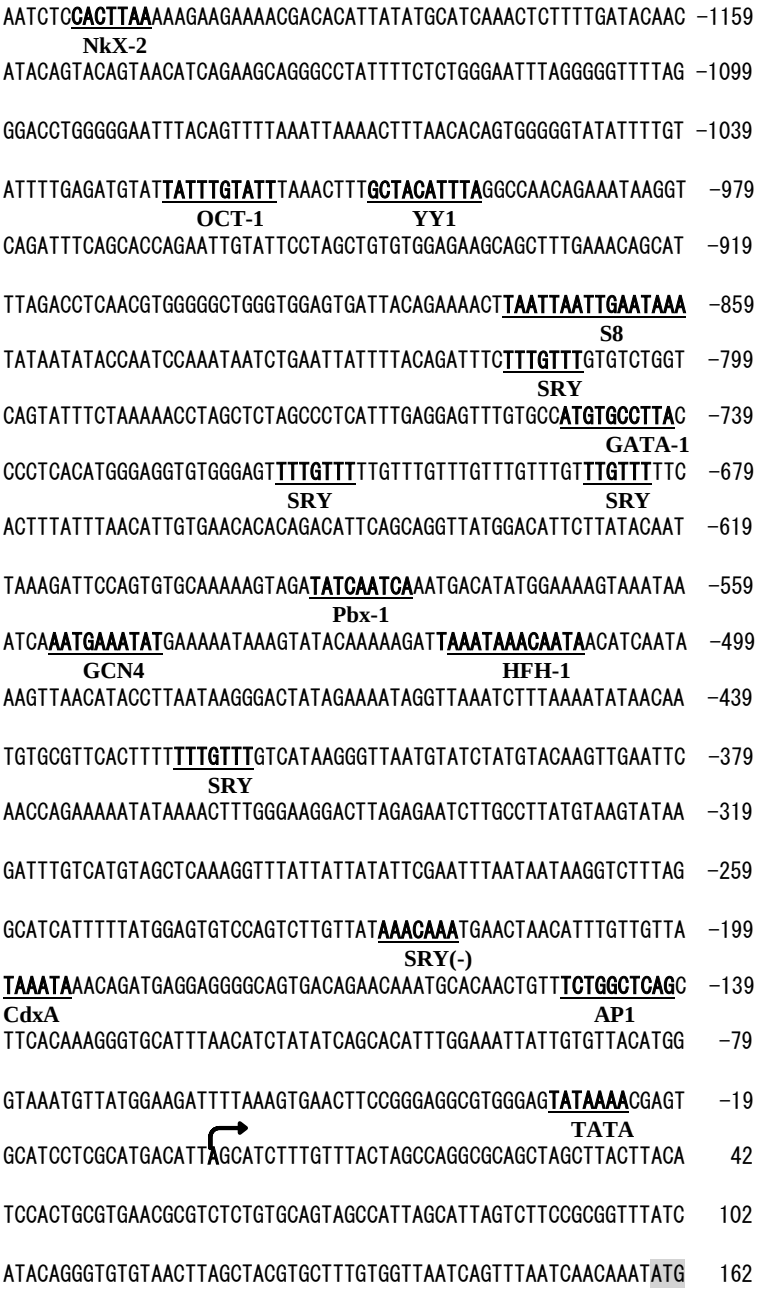

Fig. 18. **Deduced promoter region of Rbcasp3.** The transcription initiation site (+1) is denoted by a curved arrow. Putative transcription factor binding sites predicted by the TFSEARCH and Alibaba 2.1 programs are indicated by bold letters with their corresponding identity. The SRY site starts from position -417 in the sequence and is in complement form in the reverse direction.

3.3 Tertiary structural model of Rbcasp3

In order to determine the tertiary structure of pro-caspase 3 of rock bream, 3D modeling was conducted using the I-TASSER ab-initio protein prediction algorithm. The top ten caspase template crystal structures from the Research Collabratory for Structural Bioinformatis (RCSB) protein data bank used by the server exhibited over 56% identity in the threading-aligned region, with the query sequence and the Z-score values of the threading alignments exceeding 1, which ensured a considerable reliability of the predicted structure. The predicted 3D model of Rbcasp3 consisted of 5 α-helices, 21 β-strands, and 31 turns. The large and small domains, along with the linker region, resembled the typical caspase 3 structure (Rotonda et al, 1996), comprising a central hexa-stranded β-sheet with five parallel and one anti-parallel strands, a double-stranded anti-parallel β-sheet at the top of the structure, and another double-stranded anti-parallel β-sheet at the front of the molecule. Moreover, there are five helices, three on one side of the main hexa-stranded β-sheet and two on the opposite side (Fig. 19).

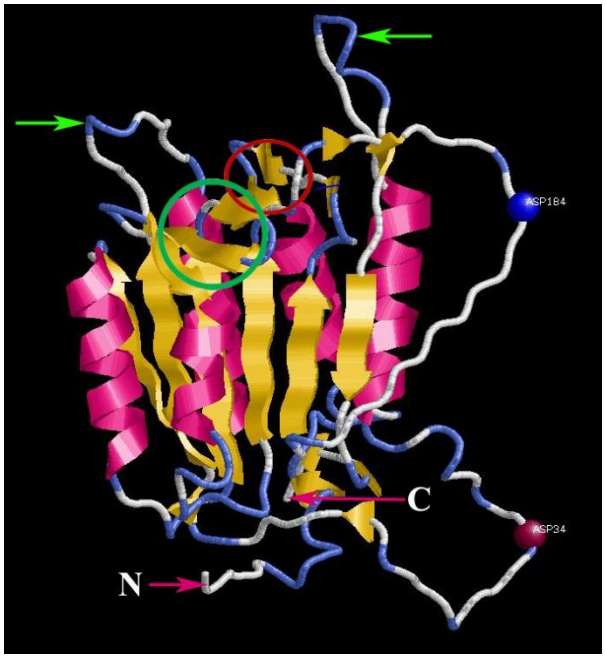

Fig. 19. Predicted 3D structural model of rock bream pro-caspase 3. Two spherical bulges (Asp 34, and Asp 184) represent the two aspartate residues where the pro-domain and the large domain is cleaved off, respectively. Green arrows indicate the two characteristic extra loops of caspase 3 architecture. β-strands are depicted in yellow and α-helices are in pink. Turns are represented in blue in the back-bone structure. Two anti-parallel double-stranded β-sheets are encircled in red and green color. The letters C and N indicate the carboxyl and amino terminals, respectively.

3.4 Recombinant expression and purification of Rbcasp3.

Rbcasp3, without the pro-domain, was sub-cloned into the pMAL-c2X vector and overexpressed under the strong tac promoter as a fusion protein with MBP in *E. coli* BL21 (DE3) cells by IPTG-driven induction. Fractions collected at different stages during the purification process of the expressed protein were visualized by SDS-PAGE (Fig. 20). The molecular mass of the purified rRbcasp3 was visually determined to be ~74 kDa, appeared as a single band. This result was compatible with the predicted molecular mass of the putative caspase 3 (~31 kDa), since the molecular mass of the MBP was around 42.5kDa.

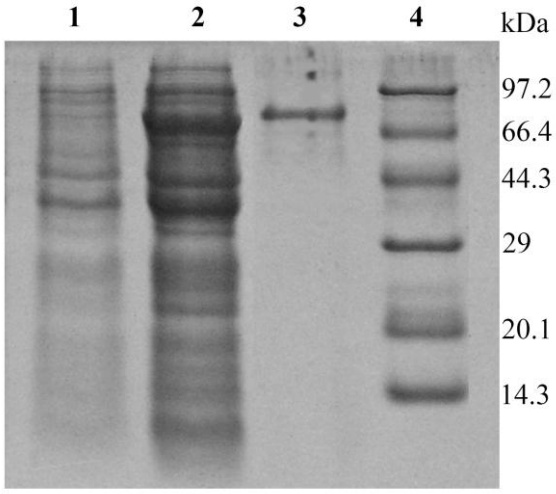

Fig. 20. SDS-PAGE analysis of overexpressed and purified recombinant Rbcasp3 fusion protein. Lane 1, total cellular extract from *E. coli* BL21 (DE3) carrying the Rbcasp3-MBP expression vector prior to IPTG induction; 2, crude extract of rRbcasp3; 3, purified recombinant fusion protein (rRbcasp3-MBP) after IPTG induction (1 mM); 4, protein markers (TaKaRa).

3.5 Hydrolyzing activity of Rbcasp3

To confirm the hydrolyzing activity of the Rbcasp3, the purified fusion protein was employed to hydrolyze the caspase 3/7-specific synthetic substrate, DEVD-*p*NA, along with the control MBP. Compared to MBP (mean A_{400}:- 0.05), rRbcasp3 exerted almost 12-fold more activity against the substrate (mean A_{400}:- 0.63), suggesting the biochemical function of Rbcasp3 while indicating comparatively low activities, against caspases 9 substrate, LEHD-*p*NA (mean A_{400}:- 0.31) and caspases 8 substrate, IETD- *p*NA (mean A_{400}:- 0.28) (Fig. 21).

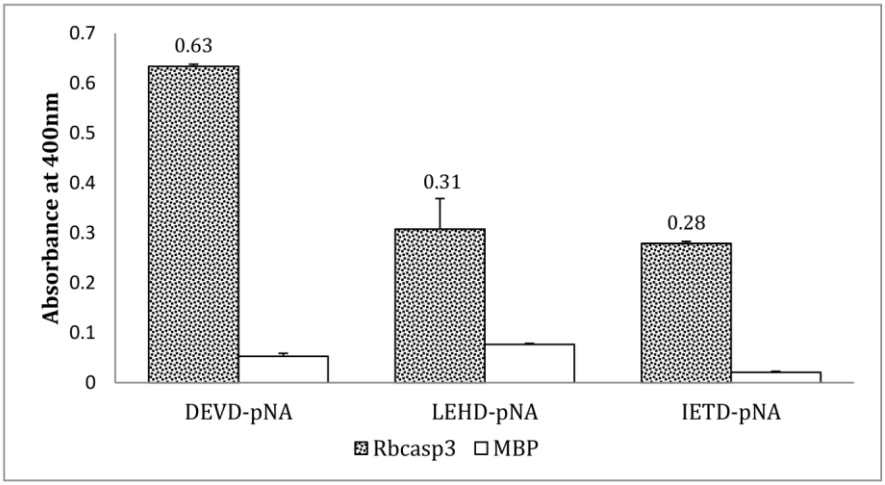

Fig. 21. *In vitro* Rbcasp3 hydrolyzing activity assay. The hydrolyzing activity against DEVD-*p*NA is represented using the corresponding absorbance value obtained at 400nm. Error bars represent the SD (n=3).

3.6 The tissue-specific expression profile of Rbcasp3

In order to determine the tissue-specific Rbcasp3 transcription profile in normal rock bream, qRT-PCR was carried out on various rock bream tissues using gene specific primers designed according to the Rbcasp3 full-length cDNA sequence. The relative expression of each tissue was obtained by comparison to expression of the rock bream β-actin gene, which was used as the non-variant internal control. To determine relative levels of tissue-specific expression, β-actin-normalized expression of each tissue was further normalized to that in the muscle (Fig. 20). Rbcasp3 mRNA was found to be constitutively expressed in all tissues investigated. However, a distinct tissue-specific transcriptional profile was found, in which the Rbcasp3 transcription levels were highest in blood, moderately high ($P < 0.05$) in liver, heart and brain tissues, and considerably low ($P < 0.05$) in all other tissues analyzed (Fig. 22).

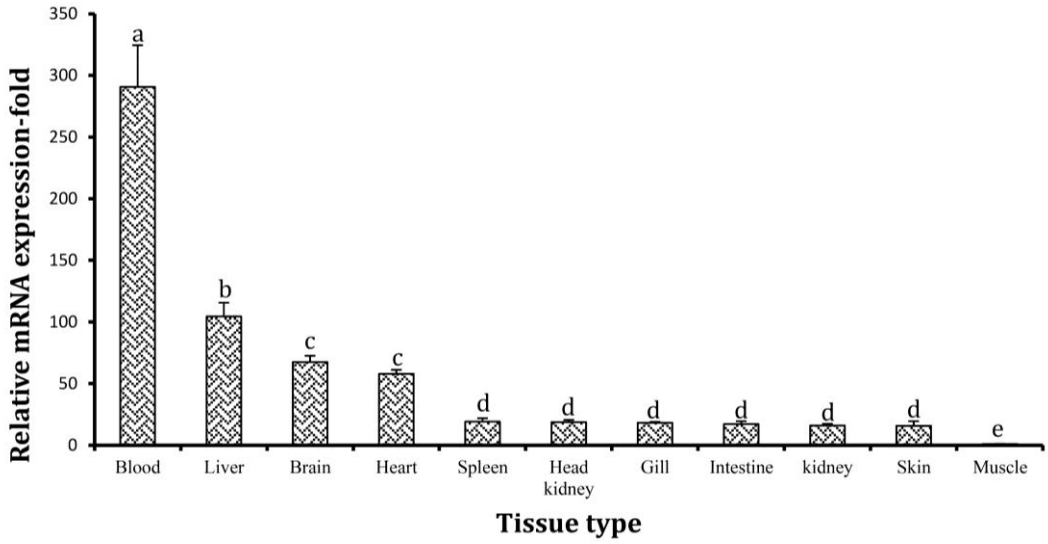

Fig. 22. Tissue expression analysis of Rbcasp3 mRNA, as determined by qRT-PCR. Error bars represent the SD (n=3) . Data with different letters are significantly different ($P<0.05$) among different tissues.

3.7 Transcriptional responses of Rbcasp3 upon immune challenges.

Liver tissue from LPS-, poly I:C-, iridovirus- and *E. tarda*-challenged rock bream was used to analyze the mRNA expression levels in response to immune stimulations. The qRT-PCR detected Rbcasp3 levels were normalized to the rock bream β-actin expression profile and compared to the transcript level detected in PBS-injected controls at each time point.

In liver cells of LPS-challenged fish, the Rbcasp3 transcript levels were significantly ($P < 0.05$) up-regulated at 12h and 24h post-injection, indicating ~2.5 fold expression increase at both time points (Fig. 23A). In contrast, liver cells of the *E. tarda*-challenged animals exhibited a significant ($P < 0.05$) and persistent up-regulation from 3h to 48h post-injection, reaching peak expression (3-fold) at 48h. However, at all the time points examined, the transcription was induced by *E. tarda* with respect to the basal level (0 h), (Fig. 23A).

As shown in the Figure 23B, at 3 h and 6 h after poly I:C injection, the Rbcasp3 transcription profile in liver cells exhibited a significant early-phase increase ($P < 0.05$) with the peak (2.6-fold) occurring at the 6 h time point. However, a subsequent down-regulation was observed at 24 h post-injection, followed by a significant late-phase increase (2.4-fold, $P < 0.05$) at 48 h post-injection. Figure 23B also depicts the differential mRNA expression profile of Rbcasp3 in liver tissue in response to the RBIV challenge. Over the experiment time course, the Rbcasp3 expression slightly fluctuated up to 24 h post-injection, followed by a significant increase (3.3-fold) at 48 h, which indicated the late-phase response to the viral-induced immune challenge.

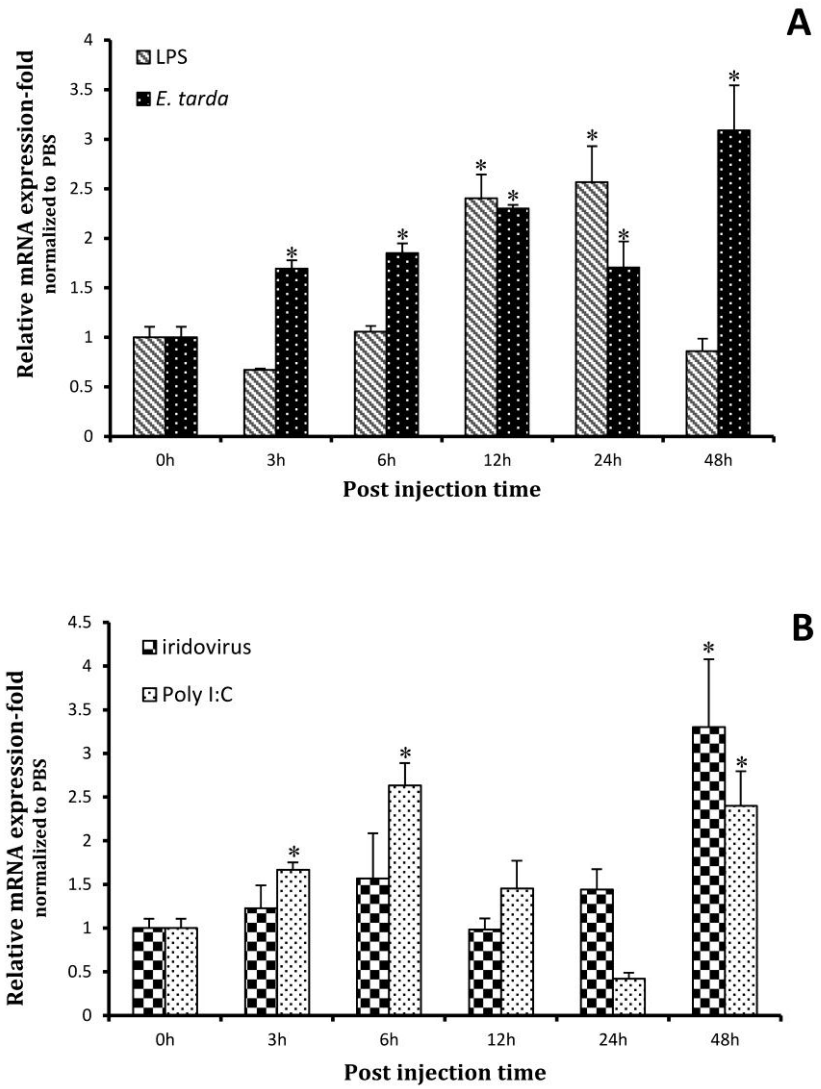

Fig.23. Expression profile of Rbcasp3 mRNA in liver tissue upon immune stimulation with (A) LPS or *E .tarda* bacteria, (B) poly I:C or iridovirus, as determined by qRT-PCR. The relative expression was calculated by the $2^{-\Delta\Delta CT}$ method using rock bream β-actin as the reference gene with respect to corresponding PBS injected controls at each time point. The relative expression fold-change at 0 h post-injection was used as the basal line. Error bars represent the SD ($n = 3$); *$P < 0.05$.

4. Discussion

Apoptosis can play a key role in defense of an organism through limiting the pool of host cells for the productive replication of pathogenic organisms such as bacteria and viruses (Chang and Yang, 2000). Caspase 3 is a pivotal regulator of the executionary phase of apoptosis, and is involved in many of the molecular mechanisms underlying programmed cell death (Gerald, 1997). Therefore, the elevated activity of caspase 3 can be considered as a useful bio-marker of cells undergoing apoptosis (Abu-Qare et al, 2001). However, information on caspase 3 in fish at the genomic level is relatively scarce. In the present study, the caspase 3 gene was identified in rock bream and characterized structurally and functionally. The rock bream species is an important member of the marine aquaculture industries in countries located in the Asia-Pacific zone. To gain a better understanding of how rock bream immunity may be modulated, transcriptional responses of the newly-identified caspase 3 homologue towards several common pathogenic microorganisms were investigated. The putative caspase 3 gene was identified from our previously established (GS-FLX^{Tm}) rock bream cDNA sequence database by using BLAST analysis. This novel gene was found to exhibit 88.8% identity with the caspase3 gene from large yellow croaker (Table 2). Moreover, the ORF (283 aa) and the predicted molecular mass of deduced amino acids of Rbcasp3 showed a higher similarity to caspase 3 molecules of other fish species and its mammalian counterparts (Fernandes-Alnemri et al, 1994; Li et al, 2011; Reis et al, 2007; Wang and Keiser, 1998; Yabu et al, 2001). The presence of characteristic domain organization (pro-domain, large subunit, and small subunit) and the predominant features of caspase family signatures, such as the penta-peptide binding motif, the protein binding domain (GSWFI), RGD motif, and critical amino acid residues in the catalytic center and binding pocket lent credence to the hypothesis that Rbcasp3 was indeed a caspase 3 homologue (Fig. 17).

The predicted genomic structure of Rbcasp3 shares similar intron/exon architecture with the caspase 3 homologues in a majority of fish species (Fig 17). However the genome structure deviates from that in the zebrafish (Ensemble ID: ENSDART00000005593), which has one more exon. This additional exon in zebrafish contains a part of the 5'-UTR, altogether using two exons for the complete 5'-UTR, and more closely resembling the human caspase 3 genomic structure (Ensemble ID: ENST00000308394). The length of each exon in rock bream caspase 3 is almost identical to the corresponding exons in sea bass, even though the gene arrangements are different with respect to their intron lengths. Interestingly, the conserved penta-peptide binding motif is interrupted by an intron after its first amino acid in all the species, serving as a unique feature of caspase 3 genome organizations.

The predicted promoter region of Rbcasp3 was determined to consist of ~1Kb sequence, which includes several putative transcription factor binding sites (Fig. 18), substantiating the notion of tight regulation of caspase gene expression. Particularly, the putative transcription factor binding sites that were identified are known to be involved in transcriptional activation (GCN4 motif) (Hope and Struhl, 1987), LPS-induced signaling (AP-1) (Guha and Mackman, 2001), virus-induced cell signaling (OCT-1) (Lee et al, 2001), and oncogenic transcriptional activation (Pbx-1) (Mazieres et al, 2005). Presence of the latter three sites suggested that the anticipated promoter region, which presumably drives the transcription of Rbcasp3 may be activated by different immune stimulants, as well as neoplastic signals.

Phylogenetic analysis of Rbcasp3 indicated that fish and mammalian sub-clusters are independently clustered into a vertebrate clade (Fig 16). Furthermore the tree revealed that Rbcasp3 is phylogenetically more close to caspase 3B isoform from Japanese medaka and

Atlantic salmon, rather than caspases 3A isoform from medaka, providing evidence to propose that the identified and cloned novel Rbcasp3 may be the variant B of caspases 3 in rock bream. In addition, clustering pattern indicated that caspase 3 from southern house mosquito and pacific white shrimp share a common ancestor, supporting the close evolutionary relationship of caspase 3 in insects and crustaceans.

Our computational-based attempt to determine the tertiary structure of rock bream pro-caspase 3 (Fig.19) generated the distinctive caspase 3 structure, with regard to the known large and small domains of human caspase 3 (Fernandes-Ainmeri etal, 1994). As described in the results section, the 3D model was comprised of corresponding β-sheets, α-helices, and extra loops with respect to the relevant positions, corroborating the existence of the novel rock bream pro-caspase 3.

Caspases are known to be active as tetramers, consisting of large and small subunit heterodimers, after proteolysis. Furthermore this proteolysis can be occurred through auto activation, transactivation or by other proteinases. However in previous studies, it was demonstrated that caspases can show low, but detectable activity as non-processed pro-enzymes (Wolf and Green et al, 1999) According to the SDS-PAGE analysis, purified rRbcasp3 was appeared as a single band, directing us to conclude that after purification the recombinant caspases 3 has not been auto-processed.

The hydrolyzing activity assay with rRbcasp3 fusion protein showed a substantial activity relative to the control MBP, against the mammalian caspase 3/7-specific substrate, DEVD-*p*NA (Fig. 21). This finding indicated that Rbcasp3 harbors the typical biochemical property of caspase 3, affirming the functional similarly of Rbcasp3 with known members of the caspase 3 subfamily. Moreover, compared to the activity detected against caspases 9 (LEHD-*p*NA) and caspase 8 substrate (IETD-*p*NA), Rbcasp3 exerted a noticeable

specificity against caspase 3/7 substrate, DEVD-*p*NA (Fig. 21). However, low but detectable activity; exerted by Rbcasp3 against non caspases 3/7 substrates may be attributed with multi-substrate tolerable property of caspases 3 molecules, in certain extend (Fang et al, 2006).

According to the qRT-PCR analyses, caspase 3 transcription was detectable in every rock bream tissue tested, to varying degree (Fig. 22). The highest expression level was detected in blood, whereas the lowest was detected in muscle. This pattern was in agreement with that shown in a previous study of caspase 3 in large yellow croaker (Li et al, 2011). Similarly, the rock bream expression pattern was consistent with that in sea bass, whereby moderately higher transcription level was observed in heart and relatively low levels were detected in spleen, intestine, and head kidney (Reis et al, 2007). However, in rock bream, the second most abundant expression of caspase 3 was detected in liver, which is a potent immune-related organ involved in host defense (Seki et al, 2000; Sheth et al, 2001), although it was found to be much lower in sea bass and large yellow croaker (Li et al, 2011; Reis et al, 2007). In mammalian tissues, caspase 3 mRNA expression is more or less compatible with the expression patterns reported for fish. Evaluation of mRNA expression of rat caspase 3 exhibited an omnipresent expression in every tissue tested, with remarkably predominant levels in spleen, kidney, thymus and lung (Juan et al, 1996). Moreover, mouse caspase 3 transcription was abundantly detected in spleen, but scarcely detected in brain, lung, liver, and kidney (Juan et al, 1996). Hence, the ubiquitous expression of caspase 3 mRNA in various immune-related tissues of different organisms supports the notion that caspase 3 can play a significant role in host immunity.

In order to investigate the potential of apoptosis in rock bream liver tissues as an immune-related responses to viral and bacterial infections, Rbcasp3 gene expression was evaluated

by qRT-PCR during challenges with *E. tarda*, a gram-negative bacteria, and LPS, a well-characterized endotoxin in the cell wall of gram-negative bacteria as well as with iridovirus, a virulent pathogen for rock bream, and poly I:C, a pathogen-associated molecular pattern (PAMP) that emulates the double-stranded viral DNA. The transcriptional response to *E. tarda* challenge revealed that Rbcasp3 is a candidate gene for bacterial induction. At all the time points between 3 h and 48 h post-injection, Rbcasp3 was significantly up-regulated reaching its peak at 48h (Fig. 23A). This observation is in agreement with the induction pattern reported for sea bass upon *phdp* stimulation (Reis et al, 2007) and that detected during trivalent bacterial vaccine challenge in large yellow croaker (Li et al, 2011). However, in our LPS challenge, significant Rbcasp3 up-regulation was only noticed at two time points: 12 h and 24 h post-injection, which would be considered late-responses, as compared to *E. tarda* induction. This may due to the different forms of the bacterial stimulants used in both experiments. Since *E. tarda* is a live pathogenic bacterium, it can instigate a relatively strong immune response, as compared to LPS injection, which is a nonliving chemical component isolated from the bacterial cell wall. According to the viral challenges, Rbcasp3 exhibited significant up-regulation in response to both poly I:C and iridovirus. The poly I:C elicited a rapid response (3 h and 6 h post-injection) (Fig. 23B). The difference in the above two responses may be attributed to the different PAMP markers inducing corresponding receptors on the host immune cells. Altogether, these results suggest that temporal transcriptional modulations of caspase 3 in rock bream, involved in apoptotic cascade, can be triggered by bacterial and viral infections.

In summary, the full-length cDNA and the genomic DNA sequences of rock bream caspase 3 gene were identified from the previously established cDNA and genomic DNA libraries, respectively. Structural and functional characterization was carried out, along

with analyzed of the transcriptional variations in healthy and immune-challenged fish. Phylogenetic analysis revealed the prominent evolutionary relationships of Rbcasp3 with other vertebrate species, especially with fish. Bioinformatics analysis of the predicted promoter region provided initial insights into the regulatory factors of Rbcasp3 expression. Moreover, recombinant caspase 3 protein displayed protease properties against its specific substrate, substantiating its functional viability. The immune response of Rbcasp3 gene expression upon viral and bacterial challenges provided evidence of the involvement of caspase 3 in viral and bacterial defense in rock bream. Future research investigating the dynamic contribution of caspase 3 in rock bream may help to solve the pathogenic threat on the fish.

References

Abu-Qare, A.W., Abou-Donia, M.B., 2001. Biomarkers of apoptosis: release of cytochrome c, activation of caspase-3, induction of 8-hydroxy-2'-deoxyguanosine, increased 3-nitrotyrosine, and alteration of p53 gene. J Toxicol Environ Health B Crit Rev 4, 13-32.

Avunje, S., Kim, W.S., Park, C.S., Oh, M.J., Jung, S.J., 2011. Toll-like receptors and interferon associated immune factors in viral haemorrhagic septicaemia virus-infected olive flounder (Paralichthys olivaceus). Fish shellfish immunol 31, 407-414.

Baoprasertkul, P., Peatman, E., Abernathy, J., Liu, Z., 2007. Structural characterisation and expression analysis of toll-like receptor 2 gene from catfish. Fish shellfish immunol 22, 418-426.

Bell, J.K., Mullen, G.E., Leifer, C.A., Mazzoni, A., Davies, D.R., Segal, D.M., 2003. Leucine-rich repeats and pathogen recognition in Toll-like receptors. Trends Immunol 24, 528-533.

Bradford M.M., 1976. A rapid and sensitive method for the quantitation of microgram quantities of protein utilizing the principle of protein-dye binding. Anal Biochem 72, 248-254.

Bricknell, I., Dalmo, R.A., 2005. The use of immunostimulants in fish larval aquaculture. Fish & shellfish immunol 19, 457-472.

Cohen, G.M., 1997. Caspases: the executioners of apoptosis. Biochem J 326, 1-16.

Danial, N.N., Korsmeyer, S.J., 2004. Cell death: critical control points. Cell 116, 205-219.

De Oliveira, N.F., Andia, D.C., Planello, A.C., Pasetto, S., Marques, M.R., Nociti, F.H., Jr., Line, S.R., De Souza, A.P., 2011. TLR2 and TLR4 gene promoter methylation status during chronic periodontitis. J Clin Periodontol 38, 975-983.

Deveraux, Q.L., Reed JC., 1999. IAP family proteins--suppressors of apoptosis. Genes Dev 13, 239-252.

Earnshaw, W.C., Martins, L.M., Kaufmann, S.H., 1999. Mammalian caspases: structure, activation, substrates, and functions during apoptosis. Annu Rev Biochem 68, 383-424.

Elmore, S., 2007. Apoptosis: a review of programmed cell death. Toxicol Pathol. 35, 495-516.

Everett, H., McFadden, G., 1999 Apoptosis: an innate immune response to virus infection. Tren Micro Biol 7, 160-165.

Fang B., Boross P.I., Tozser, J, Weber I.T., 2006. Structural and kinetic analysis of caspase-3 reveals role for s5 binding site in substrate recognition. J Mol Biol, 360 654-666.

Fernandes-Alnemri, T., Litwack, G., Alnemri, E.S., 1994. CPP32, a novel human apoptotic protein with homology to Caenorhabditis elegans cell death protein Ced-3 and mammalian interleukin-1 beta-converting enzyme. J Biol Chem 269, 30761-30764.

Fuentes-Prior, P., Salvesen G.S., 2004. The protein structures that shape caspase activity, specificity, activation and inhibition. Biochem J 384, 201-232.

Ganesan, R., Mittl, P.R., Jelakovic, S., Grütter, M.G., 2006. Extended substrate recognition in caspase-3 revealed by high resolution X-ray structure analysis. J Mol Biol 359, 1378-1388.

Gerald, M., 1997. Caspases: the executioners of apoptosis. Biochem. J Rev 326, 1-16.

Guha, M., Mackman, N., 2001. LPS induction of gene expression in human monocytes. Cell Signal 13, 85-94.

Hadley, J.S., Wang, J.E., Foster, S.J., Thiemermann, C., Hinds, C.J., 2005. Peptidoglycan of Staphylococcus aureus upregulates monocyte expression of CD14, Toll-like receptor 2 (TLR2), and TLR4 in human blood: possible implications for priming of lipopolysaccharide signaling. Infect Immun 73, 7613-7619.

Hansen, J.D., Vojtech, L.N., Laing, K.J., 2011. Sensing disease and danger: a survey of vertebrate PRRs and their origins. Dev Comp Immunol 35, 886-897.

Hengartner, M.O., 2000. The biochemistry of apoptosis. Nature 407, 770-776.

Hess, J., Angel, P., Schorpp-Kistner, M., 2004. AP-1 subunits: quarrel and harmony among siblings. J Cell Sci 117, 5965-5973.

Hirono, I., Takami, M., Miyata, M., Miyazaki, T., Han, H.J., Takano, T., Endo, M., Aoki, T., 2004. Characterization of gene structure and expression of two toll-like receptors from Japanese flounder, Paralichthys olivaceus. Immunogenetics 56, 38-46.

Hirschfeld, M., Weis, J.J., Toshchakov, V., Salkowski, C.A., Cody, M.J., Ward, D.C., Qureshi, N., Michalek, S.M., Vogel, S.N., 2001. Signaling by toll-like receptor 2 and 4 agonists results in differential gene expression in murine macrophages. Infect Immun 69, 1477-1482.

Hope, I.A., Struhl, K., 1987. GCN4, a eukaryotic transcriptional activator protein, binds as a dimer to target DNA EMBO J 6, 2781-2784.

Ho, PK., Hawkins, C.J., 2005. Mammalian initiator apoptotic caspases FEBS J 272, 5436-5453.

Igney, F.H., Krammer, P.H., 2002. Death and anti-death: tumour resistance to apoptosis. Nature reviews. Cancer 2, 277-288.

Jault, C., Pichon, L., Chluba, J., 2004. Toll-like receptor gene family and TIR-domain adapters in Danio rerio. Mol immunol 40, 759-771.

Jin, M.S., Kim, S.E., Heo, J.Y., Lee, M.E., Kim, H.M., Paik, S.G., Lee, H., Lee, J.O., 2007. Crystal structure of the TLR1-TLR2 heterodimer induced by binding of a tri-acylated lipopeptide. Cell 130, 1071-1082.

Johnson, A.L., Bridgham, J.T., 2000. Caspase-3 and -6 expression and enzyme activity in hen granulosa cells. Biol Reprod 62, 589-598.

Juan, T.S., McNiece, I.K., Jenkins, N.A., Gilbert, D.J., Copeland, N.G., Fletcher, F.A., 1996. Molecular characterization of mouse and rat CPP32 beta gene encoding a cysteine protease resembling interleukin-1 beta converting enzyme and CED-3. Oncogene 13, 749-755.

Kerr, J.F., Wyllie, A.H., Currie, A.R., 1972. Apoptosis: a basic biological phenomenon with wide-ranging implications in tissue kinetics. Br J Cancer 26, 239-257.

Kumar, S., Tamura, K., Nei, M., 2004. MEGA3: Integrated software for Molecular Evolutionary Genetics Analysis and sequence alignment. Brief Bioinform 5, 150-163.

Lacroix, I., Lipcey, C., Imbert, J., Kahn-Perles, B., 2002. Sp1 transcriptional activity is up-regulated by phosphatase 2A in dividing T lymphocytes. J Biol Chem 277, 9598-9605.

Lavrik, I.N., Golks, A., Krammer, P.H., 2005. Caspases: pharmacological manipulation of cell death. J Clin Invest 115, 2665-2672.

Lee, L., Stollar, E., Chang, J., Grossmann, J.G., O'Brien, R., Ladbury, J., Carpenter, B., Roberts, S., Luisi, B., 2001. Expression of the Oct-1 transcription factor and characterization of its interactions with the Bob1 coactivator. Biochem 40, 6580-6588.

Livak, K.J., Schmittgen, T.D., 2001. Analysis of relative gene expression data using real-time quantitative PCR and the 2(-Delta Delta C(T)) Method. Methods 25, 402-408.

Liedtke, C., Groger, N., Manns, M.P., Trautwein, C., 2003. The human caspase-8 promoter sustains basal activity through SP1 and ETS-like transcription factors and can be up-regulated by a p53-dependent mechanism. J Biol Chem 278, 27593-27604.

Li, M., Ding, Y., Mu, Y., Ao, J., Chen, X., 2011. Molecular cloning and characterization of caspase-3 in large yellow croaker (*Pseudosciaena crocea)*. Fish Shellfish Immunol 30, 910-916.

Liu, W., Wang, G., Yakovlev, A.G., 2002. Identification and functional analysis of the rat caspase-3 gene promoter. J Biol Chem 277, 8273-8278.

Magnadottir, B., 2006. Innate immunity of fish (overview). Fish shellfish immunol 20, 137-151.

Martin, M.U., Wesche, H., 2002. Summary and comparison of the signaling mechanisms of the Toll/interleukin-1 receptor family. Biochimica et biophysica acta 1592, 265-280.

Mazieres, J., You, L., He, B., Xu, Z., Lee, A.Y., Mikami, I., McCormick, F., Jablons, D.M., 2005. Inhibition of Wnt16 in human acute lymphoblastoid leukemia cells containing the translocation induces apoptosis. Oncogene 24, 5396-5400.

Meijer, A.H., Gabby Krens, S.F., Medina Rodriguez, I.A., He, S., Bitter, W., Ewa Snaar-Jagalska, B., Spaink, H.P., 2004. Expression analysis of the Toll-like receptor and TIR domain adaptor families of zebrafish. Mol immunol 40, 773-783.

Miao, E.A., Leaf, I.A., Treuting, P.M., Mao, D.P., Dors, M., Sarkar, A., Warren, S.E., Wewers, M.D., Aderem A., 2010. Caspase-1-induced pyroptosis is an innate immune effector mechanism against intracellular bacteria. Nat Immunol 11, 1136-1142.

Naruse, K., Fukamachi, S., Mitani, H., Kondo, M., Matsuoka, T., Kondo, S., Hanamura, N., Morita, Y., Hasegawa, K., Nishigaki, R., Shimada, A., Wada, H., Kusakabe, T., Suzuki, N., Kinoshita, M., Kanamori, A., Terado, T., Kimura, H., Nonaka, M., Shima, A., 2000. A detailed linkage map of medaka, Oryzias latipes: comparative genomics and genome evolution. Genetics 154, 1773-1784.

Nicholson, D.W., 1999. Caspase structure, proteolytic substrates, and function during apoptotic cell death. Cell Death Differ 6, 1028-1042.

Nicholson, D.W., Thornberry, N.A., 1997. Caspases: killer proteases. Trends Biochem Sci 22, 299-306.

Norbury, C.J., Hickson, I.D., 2001. Cellular responses to DNA damage. Annu Rev Pharmacol Toxicol 41, 367-401.

O'Connell, C.M., Ionova, I.A., Quayle, A.J., Visintin, A., Ingalls, R.R., 2006. Localization of TLR2 and MyD88 to Chlamydia trachomatis inclusions. Evidence for signaling by intracellular TLR2 during infection with an obligate intracellular pathogen. J Biol Chem 281, 1652-1659.

O'Neill, L.A., Bowie, A.G., 2007. The family of five: TIR-domain-containing adaptors in Toll-like receptor signalling. Nat Rev Immunol 7, 353-364.

Oshiumi, H., Matsuo, A., Matsumoto, M., Seya, T., 2008. Pan-vertebrate toll-like receptors during evolution. Curr genomics 9, 488-493.

Oshiumi, H., Tsujita, T., Shida, K., Matsumoto, M., Ikeo, K., Seya, T., 2003. Prediction of the prototype of the human Toll-like receptor gene family from the pufferfish, Fugu rubripes, genome. Immunogenetics 54, 791-800.

Palti, Y., 2011. Toll-like receptors in bony fish: from genomics to function. Dev Comp Immunol 35, 1263-1272.

Park, S.I., 2009. Disease conrtol in Korean aquaculture. Fish Pathol 44, 19-23.

Parrott, C., Seidner, T., Duh, E., Leonard, J., Theodore, T.S., Buckler-White, A., Martin, M.A., Rabson, A.B., 1991. Variable role of the long terminal repeat Sp1-binding sites in human immunodeficiency virus replication in T lymphocytes. J Virol 65, 1414-1419.

Pierschbacher, M.D., Ruoslahti, E., 1984. Cell attachment activity of fibronectin can be duplicated by small synthetic fragments of the molecule. Nature 309, 30-33.

Rebl, A., Goldammer, T., Seyfert, H.M., 2010. Toll-like receptor signaling in bony fish. Vet Immunol Immunopathol 134, 139-150.

Reese, M.G., 2001. Application of a time-delay neural network to promoter annotation in the Drosophila melanogaster genome. Computers & chemistry 26, 51-56.

Reis, M.I., Nascimento, D.S., do Vale, A., Silva, M.T., dos Santos, N.M., 2007. Molecular cloning and characterisation of sea bass (*Dicentrarchus labrax L.*) caspase-3 gene. Mol Immunol 44, 774-783.

Ribeiro, C.M., Hermsen, T., Taverne-Thiele, A.J., Savelkoul, H.F., Wiegertjes, G.F., 2010. Evolution of recognition of ligands from Gram-positive bacteria: similarities and differences in the TLR2-mediated response between mammalian vertebrates and teleost fish. J immunol 184, 2355-2368.

Roach, J.C., Glusman, G., Rowen, L., Kaur, A., Purcell, M.K., Smith, K.D., Hood, L.E., Aderem, A., 2005. The evolution of vertebrate Toll-like receptors. Proceedings of the National Academy of Sciences of the United States of America 102, 9577-9582.

Rotonda, J., Nicholson, D.W., Fazil, K.M., Gallant, M., Gareau, Y., Labelle, M., Peterson, E.P., Rasper D.M., Ruel, R., Vaillancourt, J.P., Thornberry, N.A., Becker, J.W., 1996. The three-dimensional structure of apopain/CPP32, a key mediator of apoptosis. Nat Struct Biol 3 619-625.

Samanta, M., Swain, B., Basu, M., Panda, P., Mohapatra, G.B., Sahoo, B.R., Maiti, N.K., 2012. Molecular characterization of toll-like receptor 2 (TLR2), analysis of its inductive expression and associated down-stream signaling molecules following ligands exposure and bacterial infection in the Indian major carp, rohu (*Labeo rohita*). Fish shellfish immunol 32, 411-425.

Seki, S., Habu, Y., Kawamura, T., Takeda, K., Dobashi, H., Ohkawa, T., Hiraide, H., 2000. The liver as a crucial organ in the first line of host defense: the roles of Kupffer cells, natural killer (NK) cells and NK1.1 Ag+ T cells in T helper 1 immune responses. Immunol Rev 174, 35-46.

Sheth, K., Bankey, P., 2001. The liver as an immune organ. Curr Opin Crit Care 7, 99-104.

Slack, J.L., Schooley, K., Bonnert, T.P., Mitcham, J.L., Qwarnstrom, E.E., Sims, J.E., Dower, S.K., 2000. Identification of two major sites in the type I interleukin-1 receptor cytoplasmic region responsible for coupling to pro-inflammatory signaling pathways. J Biol Chem 275, 4670-4678.

Sun, E.W., Shi, Y.F., 2001. Apoptosis: the quiet death silences the immune system. Pharmacol Ther 92, 135-145.

Takle, H., McLeod, A., Andersen, O., 2006. Cloning and characterization of the executioner caspases 3, 6, 7 and Hsp70 in hyperthermic Atlantic salmon (*Salmo salar*) embryos. Comp Biochem Physiol B Biochem Mol Biol 144, 188-198.

Tamura, K., Dudley, J., Nei, M., Kumar, S., 2007. MEGA4: Molecular Evolutionary Genetics Analysis (MEGA) software version 4.0. Mol Biol Evol 24,1596-1599.

Tarantino, G., Savastano, S., Capone, D., Colao, A., 2011. Spleen: A new role for an old player? World journal of gastroenterology : WJG 17, 3776-3784.

Thornberry, N.A., Lazebnik, Y., 1998. Caspases: enemies within. Science 281 1312-1316.

Tian, B., Brasier, A.R., 2003. Identification of a nuclear factor kappa B-dependent gene network. Recent progress in hormone research 58, 95-130.

Underhill, D.M., Ozinsky, A., Hajjar, A.M., Stevens, A., Wilson, C.B., Bassetti, M., Aderem, A., 1999. The Toll-like receptor 2 is recruited to macrophage phagosomes and discriminates between pathogens. Nature 401, 811-815.

Wang, H., Keiser, J.A., 1998. Molecular characterization of rabbit CPP32 and its function in vascular smooth muscle cell apoptosis. Am J Physiol 274, 1132-1140.

Wei, Y.C., Pan, T.S., Chang, M.X., Huang, B., Xu, Z., Luo, T.R., Nie, P., 2011. Cloning and expression of Toll-like receptors 1 and 2 from a teleost fish, the orange-spotted grouper Epinephelus coioides. Vet Immunol Immunopathol 141, 173-182.

Werling, D., Jungi, T.W., 2003. TOLL-like receptors linking innate and adaptive immune response. Vet Immunol Immunopathol 91, 1-12.

Werts, C., Tapping, R.I., Mathison, J.C., Chuang, T.H., Kravchenko, V., Saint Girons, I., Haake, D.A., Godowski, P.J., Hayashi, F., Ozinsky, A., Underhill, D.M., Kirschning, C.J., Wagner, H., Aderem, A., Tobias, P.S., Ulevitch, R.J., 2001. Leptospiral lipopolysaccharide activates cells through a TLR2-dependent mechanism. Nat immunol 2, 346-352.

Wolf, B.B., Green, D.R., 1999. Suicidal tendencies: apoptotic cell death by caspase family proteinases. J Biol Chem 274, 20049-20052.

Xagorari, A., Chlichlia, K., 2008. Toll-like receptors and viruses: induction of innate antiviral immune responses. Open Microbiol J 2, 49-59.

Xu, Y., Tao, X., Shen, B., Horng, T., Medzhitov, R., Manley, J.L., Tong, L., 2000. Structural basis for signal transduction by the Toll/interleukin-1 receptor domains. Nature 408, 111-115.

Yabu, T., Kishi, S., Okazaki, T., Yamashita, M., 2001. Characterization of zebrafish caspase-3 and induction of apoptosis through ceramide generation in fish fathead minnow tailbud cells and zebrafish embryo. Biochem J 360, 39-47.

Zenke, K., Kim, K.H., 2008. Functional characterization of the RNase III gene of rock bream iridovirus. Arch Virol 153, 1651-1656

AKNOWLEDGMENT

'Dedication is the path to success'. This is a well-known saying, which has always driven my life to the victories, achieved to date and inspired me to stand on my feet in harsh circumstances. I am glade to have a supervisor in my graduate studies, who exactly follows this motto. I take this opportunity to award my sincere gratitude to Prof. Jehee Lee, my direct supervisor, for offering me an opportunity to study in Jeju National University and pursue my graduate studies under his kind guidance and encouragement in Marine Molecular Genetic laboratory. The innovative way which you have used to bloom the scientific thinking in minds of budding scientists cannot be easily estimated sir ! I will always be indebted to Dr. Ilson Whang for her valuable cooperation in my research work as well as in my publications. Moreover, I would like to express my honor to Prof. Ki-young Kim in Department of Marine Life Science for the facts on immunology taught in his course works, related to my research studies. I am also grateful to Prof. Choon Bok Song and Prof. Jun-Bum Jung for being members of my thesis committee.

My Special thanks go to Mr. Ajith Premachandra and Ms. Saranya Revathy for their valuable cooperation and logical instructions for the progress of my research performance. Further, I do not forget to acknowledge all of my lab members, including Dr. Youngdeuk Lee, Sukkyoung Lee, Hyowan Kim, Minyoung Oh, Yucheol Kim, Qiang Wan, Niroshana Wicramaaracchi, Sanjaya Bathige and Umasuthan for their kind corporation to drive my research works to a success. I am also grateful to my other Sri Lankan colleagues in my department, Kalpa Samarakoon, Dr. Janaka Wijesinghe and Prasad Rajapaksha for sharing their experience with me which in turn advanced my analytical thinking.

Finally, I gratefully mention the National Fisheries Research and Development Institute and Brain Korea 2012 program which funded my research works.